Institute of Space and Aeronautical Science, University of Tokyo
Report No. 439, May 1969

Experimental Study of the Hypersonic Rarefied Gas Flow past a Flat Plate and Around a Cylinder

By

Yasunori KOBAYASHI

Summary: Detailed flow survey around a flat plate with a sharp leading edge and a circular cylinder in the hypersonic rarefied gas flow was carried out over a wide range of the flow density. The experimental condition of the flat plate covers the range of the rarefaction parameter up to 20, and the measured results bridge the regions predictable by the strong interaction theory and by the free molecule theory. The rarefied flow around the cylinder was obtained up to the Knudsen number of 400. The so-called "shoulder wave" was found to exist in the region between the free molecule flow and the continuum flow. The structure of the wake measured is surprisingly similar to the one predicted by the viscous theory.

SYMBOLS

A: cryo-panel area or nozzle sectional area
a: accommodation coefficient
A_e: effective nozzle exit area
C: capture coefficient
C_∞: Chapman-Rubesin coefficient
D: diameter of cylinder model or probe
d: orifice diameter of pressure probe
$\mathscr{D}$: ratio of the diameter to length of the pressure probe (d/l)
e: charge of electron
f_0: function of hot-wire resistance with no flow
f: function of hot-wire resistance with flow
h_w: heat transfer coefficient
I: heat current of hot wire
j: current density to Langmuir probe
K: thermal conductivity
K_n: Knudsen number
K_w: non-dimensional heat transfer parameter
k: Boltzmann constant
l: length of the pressure probe or the hot wire
M: molecular mass of gas or Mach number
M_∞: free stream Mach number

m: particle mass
N: particle number density
P_{im}: impact pressure
P_j: measured pressure in the orifice cavity
$P_{j,or}$: pressure on the surface outside the orifice
P_r: prandtl number
P_∞: free stream static pressure
Q: heat flux
$\dot{q}$: heat transfer from flow into wall
R: gas constant
Re: Reynolds number
R: hot wire resistance
R_L: Langmuir probe radius
$S_{\max}$: specific pumping speed
S: molecular speed ratio
T: temperature
U: macroscopic mean velocity of gas
$\overline{V}_{\infty,x}$: rarefaction parameter
V_f: plasma floating potential
$\dot{V}$: actual pumping speed
$V_{\max}$: maximum volumetric pumping speed
v_m: most probable molecular speed
X: distance from leading edge to orifice of a flat plate
γ: ratio of the specific heats
ρ: density
λ: mean free path
λ_D: Debye shealding length
θ: angle which the free stream mean velocity vector makes with surface element
μ: viscosity

suffix

e: electron
i: ion
L: limit as $\lambda_w/d \to \infty$
g: gas condition
w: wall condition
∞: free stream or infinity
0: stagnation or total condition
*: nozzle throat portion

1. Introduction

Recently study of rarefield gasdynamics has made remarkable progress owing to the developments of the related techniques. The main object of this study concerns with the molecular flow or the noncontinuum character of the flow, which may be observed in a considerably low density atmosphere. The flow behavior of slightly rarefied gas is well known both experimentally and analytically, while in the case of the free molecule flow in which the flow character is predictable by the suitable analysis, the experimental investigation does not seem to be enough. The intermediate region of these two extreme cases, "transition flow region", has been left open to question due to both analytical and experimental difficulties in dealing with this region in spite of the various attempts by many researchers. In the present paper, the experimental study of the transition flow region is reported, with the emphasis of the phenomenological grasp which is the most important step to the thorough understanding of this region, and it is intended to bridge the regions predictable by the continuum flow and the free molecule theories.

The general status of the progress of rarefied gas flow study up to 1960 was summarized in [1], in which the transition flow was treated by the simple interpolation theory between the continuum flow theory which uses the Navier-Stokes equations with slight modification in the boundary condition including the slip flow effects, and the free molecule flow theory based on the gas kinetics. The recent status was surveyed more systematically in [2]. Comparing [1] and [2], one can see how remarkable progress has been made in the field of rarefied gasdynamics. Heat transfer in rarefied gas flows was also reviewed in [3].

A leading edge problem of a flat plate is the most interesting and important one in hypersonic rarefied gasdynamics, since it includes all the basic phenomena inherent to the rarefied gas flow, and many related works have been published. As a remarkable contribution to this problem, a simple flow model in the merged layer region was proposed by Oguchi [4] in 1961. In his theory, it was assumed in this region that, although the inviscid layer disappears, the shock wave still keeps the classical Rankine-Hugoniot relation, and therefore the Navier-Stokes equations are applicable to the whole flow field. This analysis results in the solution quite similar to that around a wedge. Later, taking into account the experimental fact that slip effects should not be ignored near the leading edge region, he improved the boundary condition at the body surface so as to include the slip effects, and estimated the first order effects. The results predicted the existence of a plateau of the pressure distribution curve over the region close to the leading edge [5]. Probstein *et al.* [6] analized the flow field near the leading edge in the merged layer region using almost the same method as Oguchi's except applying the boundary condition in which were taken into account the effects of shock curvature, longitudinal transport and thickness, and wall slip at the surface. The density ratio and the tangential velocity across the shock wave, however, were assumed to be given by the Rankine-Hugoniot relation. There are many additional literatures

which deal with the rarefied flow in weak interaction region [7], using the linealized Oseen equations [8], [9], or with dissociating diatomic gas [10].

Recent experimental work in the merged layer region revealed definitely the invalidity of the thin shock assumption, which is the basis of the previous analysis, and has been followed the new methods of the theoretical analysis [14]–[18]. In 1967, Oguchi [14] treated the hypersonic flow past a flat plate in the merged layer on the basis of the Navier-Stokes equations without the thin shock assumption, in which the assumptions were made that the shock is locally straight and the local similarity concept is applicable, so that the analysis of shock structure is reduced to one-dimensional problem. The overall shock shape is constructed by patching together the locally straight shocks thus determined. The slip on the wall and the curvatures of the shock and the streamline are not taken account of, though the magnitudes of the slip velocity and the normal pressure gradient were estimated from the solution. Although this paper only provides the zeroth-order solution of the problem, it must be noted that this is the first introduction of a new concept of analysis. Later Shorenstein *et al.* [15] improved this analysis, in which the shock is assumed to be locally circular, therefore the corrections of curvature due to the lateral transport within the shock and/or due to the velocity slip at the surface are included. The prediction of these analyses is well consistent with the recent experimental results. Another new method to analyze the hypersonic viscous flow over slender bodies was reported [16], in which the basic equations valid over the entire range of continuum flow are formulated based on the Navier-Stokes equations without a priori assuming the existence of a discontinuous shock wave or an ordinary boundary layer. By this method numerical calculation can be carried out over the whole downstream region if the flow characters are given as the initial conditions at the leading edge. The reference [17] presents another new method which eliminates the thin discontinuity approximation of the conventional viscous interaction theory [19].

While, in 1961, Charwat [11] treated the leading edge problem using the kinetic near-free-molecule technique. The essence of this technique is that the "group" of undisturbed molecules with high energy collides almost tangentially with the leading edge, and causes to emit the another "group" of molecules with low mean velocity. This is called first collision. These two groups collide and formulate a new "group". This new group collides with the previous groups, called second collision, and creates another new group, and so on the collision between the groups takes place successively. He mainly discussed about the first collision, which corresponds to the near-free-molecule flow. Later, Patterson [12] pointed out the possibility of applying the free molecule gas kinetic theory to the rarefied gas flow analysis. And recently Bird [13] conducted the numerical experiment using the Monte Carlo method. However, the Kinetic treatments of this problem are rather few comparing to the contiuum treatments.

Many experimental works [20]–[36] of this problem have been reported. Schaaf *et al.* [21] measured the induced pressure of a sharp leading edge flat plate with the insulated wall in a rarefied flow using a low density wind tunnel. They

discovered the fact that, when the hypersonic interaction parameter exceeds a certain value, the measured pressure distribution begins to deviate from the value predicted by the strong interaction theory, and suggested the existence of the slip flow. Nagamatsu *et al.* [22] measured local heat transfer rates under the cold wall condition using thin film platinum heat transfer gauge. The results revealed a plateau of the distribution of the heat transfer rate, which was also recognized later in another experiment by Vidal *et al.* [23]. Chuan *et al.* [*24*] measured the surface pressure near the leading edge and the pitot pressure distribution in the flow field, but did not find a plateau even very close to the leading edge within the order of one mean free path length. He also reported that the velocity slip up to 60% of the free stream velocity was observed near the leading edge. In [*26*], the data of the surface skin friction, the heat transfer, the static pressure, the shape of the shock layer and the pitot pressure were reported, from which a rather gentle slope of the heat transfer distribution curve is observed instead of a plateau. Recently the measurements of the surface pressure under the condition with the higher hypersonic interaction parameter have become possible using more rarefied wind tunnels and the flow field survey using the various methods have begun [*29*]–[*31*]. McCroskey *et al.* [*29*], [*30*] measured the shock shape of a sharp leading edge flat plate with the cold wall in the rarefied hypersonic flow by means of schlieren photograph, nitrogen glow discharge, pitot probe and hot wire. The main results are as follows; the shock wave is everywhere convex, the shock shape is close to the one of a 3/4 power law, and the shock profile near the leading edge actually smears. Afterwards they extended the object of investigation to the slender bodies [*31*] such as wedges and cones, and discussed the body shape effect of the rarefaction to the flow field in the rarefied flow. They invented a new measuring technique [*32*] and obtained the refined data of the flow around a sharp leading edge flat plate. Becker *et al.* [*33*] and Vas *et al.* [*34*] carried out the flow field survey and the surface pressure measurement mainly for the purpose of determining the applicable range of the strong interaction theory. Maulic *et al.* [*35*] reported the detailed measurement of the induced pressure, and Harbour *et al.* [*36*], the flow field survey with electron beam probe.

Study of the rarefied gas flow around blunt bodies [*2*] has been mainly concerning to the relations of the static pressure, the stagnation pressure, the heat transfer, the shock shape and the drag coefficient to Mach number or Reynolds number. The flow field in the stagnation region of blunt bodies in hypersonic non-rarefied flow is analyzed in detail in [*19*], but a few analytical works concerning with the rarefied gas flows appeared in the literature [*37*], [*38*]. The main difficulty of this problem is due to the fact that the rarefaction effects upon a shock layer and/or a viscous layer of the blunt bodies are so complicated that the analytical approach is almost impossible.

Kao [*39*] discussed analytically the shock layer growth due to the decrease of Reynolds number in the rarefied flows around the sphere. Bird [*13*] presented the drag coefficients of a sphere and a circular cylinder (and also a flat plate) in the near-free-molecule condition, solving the Boltzmann equation by means of Monte

Carlo method.

The analytical works of the flow around the circular cylinder appeared in [40], [41] based on free molecule flow theory; [40] treated a wake of a cylinder, and [41] is using the B-G-K model.

Some experimental contributions are found in [42]–[45]. Potter *et al.* [42] measured the impact pressure in the stagnation region of the models of the hemispherical or flat nose with axisymmetric afterbody. The result indicated that the impact pressure firstly decreases with decreasing Reynolds number and then increases afterwards, and that this trend is independent of the surface temperature. Tirumalesa [44] conducted local measurements of the rotational temperature and the density around a cooled hemisphere-cylinder model set parallel to the flow using electron beam technique. Coudeville *et al.* [46] obtained the drag coefficients of cylinder models over the low speed to the supersonic flow conditions. Zapata *et al.* [47] showed the strong effect of Reynolds number to the measured surface pressure of the cylinder. Broadwell *et al.* [48] measured the shock structure, especially the shock thickening and the shock formation processes in the relation with the change of the Knudsen number.

It seems that the study of the hypersonic rarefied flow around blunt bodies has been left behind both experimentally and analytically that of a sharp edged flat plate.

In the present paper, measurements of the surface pressure and flow field survey by the several probes were conducted in the hypersonic rarefied flows past a sharp leading edge flat plate and around a circular cylinder. It should be noted that, using the low density wind tunnel with cryopumping capability, the measurements were carried out in the more rarefied flow condition with the rarefaction parameter up to 20 than those above mentioned. The detailed survey of flow field was achieved by means of several types of the probes. Carbon dioxide gas was mainly used in the experiment because it has the large capture coefficient at the temperature of the nitrogen cooled cryo-panel and, therefore, the cryopump is effectively operated. Argon and nitrogen gases are also used.

This is the author's doctor thesis submitted to the Graduate School of Engineering, University of Tokyo in 1969. The auther wishes to express his sincere thanks to Dr. K. Oshima, Associate Professor of University of Tokyo, for his continuous guidance during the course of the study. Thanks are also due to Mr. K. Sugaya for his helpful assistance in conducting the experimental work. The auther also received the attentive help from Miss H. Sakurai at the stage of arranging the paper.

2. Experimental Apparatus

2.1 *Wind Tunnel*

In this experiment the low density wind tunnel of the Institute of Space and Aeronautical Science, University of Tokyo was used. The principal feature of

this tunnel is the cryopumping capability for carbon dioxide and water vapour. The main part of the cryopump consists of nitrogen cooled panels of 2 m^2 in total, and it operates at a large pumping speed of 2×10^5 l/sec per 1 m^2 cryo-surface, which is quite close to the theoretically predicted value, and covers the wide range of the chamber pressure. The diffusion pump serves as an adjunct role. The principle and the operation of the cryopumping are described in [*49*].

When a chamber condition is of free molecule, the maximum volumetric pumping speed, $\dot{V}_{max}$ of cryopump is independent of the chamber pressure and is determined by a specific pumping speed, S_{max} calculated based on the kinetic theory and by cryo-panel area, A, and expressed as

$$\dot{V}_{max}=S_{max}\times A\ ,$$

where

$$S_{max}=\sqrt{\frac{RT_g}{2\pi M}}\ .$$

The actual pumping speed, $\dot{V}$, is a capture coefficient, C, multiplied by the maximum speed

$$\dot{V}=C\times\dot{V}_{max}\ .$$

The value of C is given experimentally; for example, 0.63 for carbon dioxide and 0.92 for water vapour at the cryo-panel temperature of 77°K. In Fig. 1 the pumping characters of this tunnel are illustrated. The specified pumping speeds of the oil diffusion pump and the mechanical booster pump are 3000 l/sec and 300 l/sec, respectively. Two rotary pumps are provided in series with the mechanical booster pump for obtaining the suitable forepressure. The cryopumping speed shows a linear character because it is almost independent of the chamber pressure as noted before. Several experimental conditions are plotted in the figure, all of which are

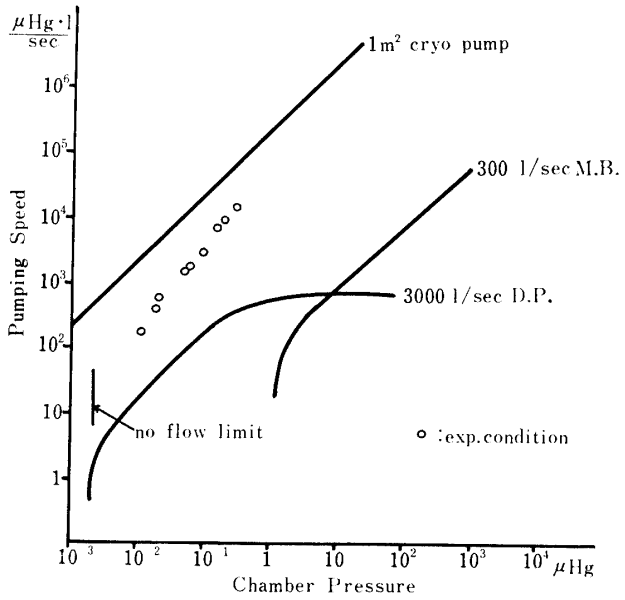

FIG. 1. Pumping performance of the wind tunnel.

beyond the capability of the diffusion pump with a reasonable size. Thus, one can see the usefulness of the cryopump.

The experimental setup is shown schematically in Fig. 2(a). The main portion is a vacuum chamber of 1.2 m in diameter and 2.4 m in length, made of wrought iron, and has glass windows of 100 mm in diameter on the both sides of the chamber at the test section. The plenum chamber is also an iron cylindrical vessel of 50 mm in internal diameter and 200 mm in length, and is fixed by the flange at one end of the vacuum chamber. The gas is fed from the bottle to the plenum chamber and the flow rate is controlled by the leak valve inserted to the feed line. The other end of the chamber is closed by the lid, which is removable in the preparation or the improvement of the test section. Nine flanges of 100 mm in diameter are provided at the top of the chamber for the terminals of the instruments, liquid nitrogen inlets or other purposes. The nozzle exit diameter is 80 mm. The nozzle throat diameter can be changed from 2 to 8 mm by exchanging the throat portion which is the small stainless steel nozzle with a given throat diameter, 16 mm exit diameter and 50 mm length. The traversing mechanism for probe survey consists of a pair of the gear systems and the survo motors, and can move the probe within the range of 200 mm both in the parallel and perpendicular directions to the flow. It can also rotate the probe. The accuracy of this mechanism is within 0.2 mm. The chamber is evacuated up to 2×10^{-6} torr

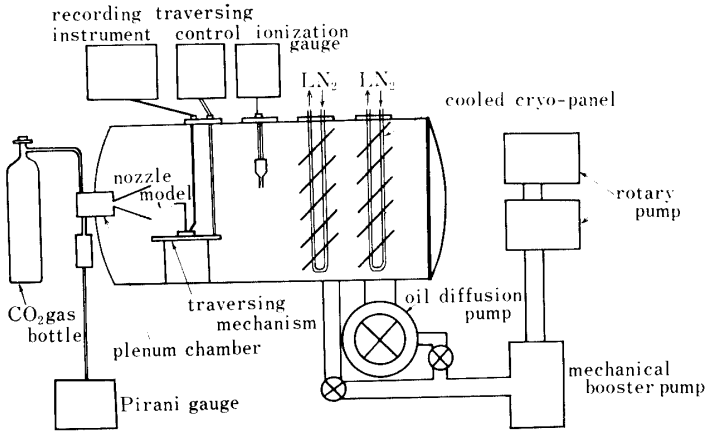

FIG. 2(a). Schematic view of the general setup

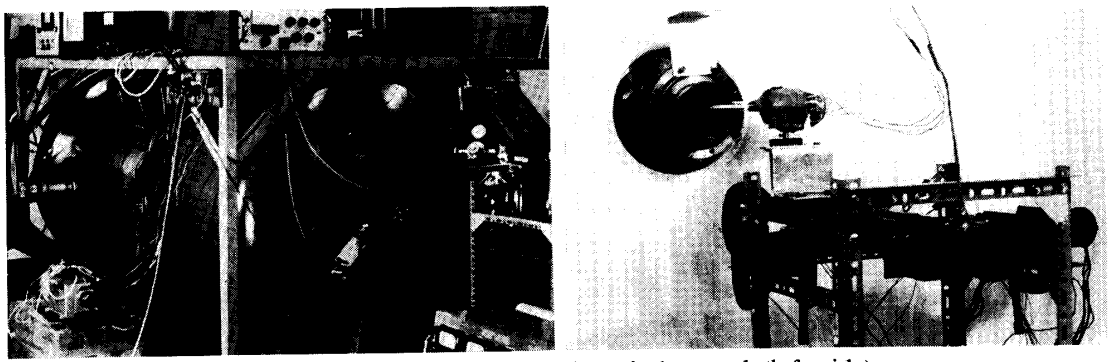

FIG. 2(b). General view of the wind tunnel (left side)
The probe traversing mechanism (right side)

under no flow condition about an hour. Liquid nitrogen for cooling the cryo-panel is fed by applying the suitable pressure of the nitrogen gas to the liquid. The cryo-panel has 1 m^2 in area and is cooled about 80°K. The photographs of the general view of the wind tunnel and the probe traversing mechanism are shown in Fig. 2(b).

The tunnel operation diagram is shown in Fig. 3. By changing the nozzle throat diameters, the tunnel can produce the flow in the range of Mach number 5 to 14, Reynolds number 10^{-2} to 1 and Knudsen number 0.1 to 400. The broken curves indicate the stagnation pressure of the plenum chamber. Definitions of the Mach number and the Reynolds number in the diagram are described in the section 2.2 Pressure Probe. The flow in the tunnel is stable and reproducible as far as the cryo-panel is kept cold below a certain temperature. The plenum and the chamber pressures are measured by the Pirani and the ionization vacuum gauges, respectively. The chamber pressure varies from 2×10^{-6} torr without flow to 5×10^{-4} torr at the maximum flow rate.

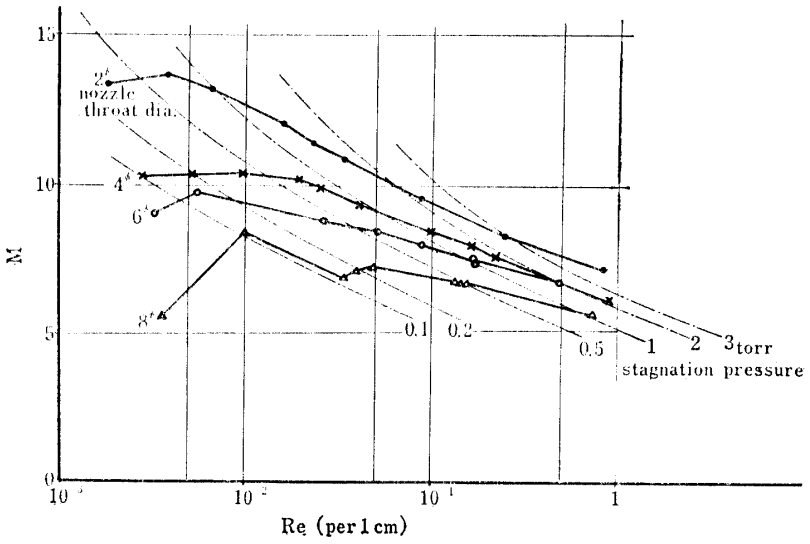

FIG. 3. Tunnel operation diagram

2.2 *Pressure Probe*

Fig. 4 shows the surveying probes used in the experiment. All the dimensions are in millimeter. The impact and the static pressure probes are made of brass and connected directly to an ionization vacuum gauge tube or to a Pirani gauge tube according to the pressure condition. The Pirani gauges for measuring of the impact or stagnation pressures were calibrated with McLeod gauge.

A square flat plate with the sharp leading edge and a long cylindrical tube were used as the bodies for investigating the flow in this experiment. These are shown in Fig. 5. The plate is provided with a reservoir of liquid nitrogen and can be uniformly cooled down to about 80°K. At 18.5 mm downward from the leading edge is located an orifice for surface pressure measurement, and the vacuum gauge is fixed directly to it as is the case with the other pressure probes. The flat

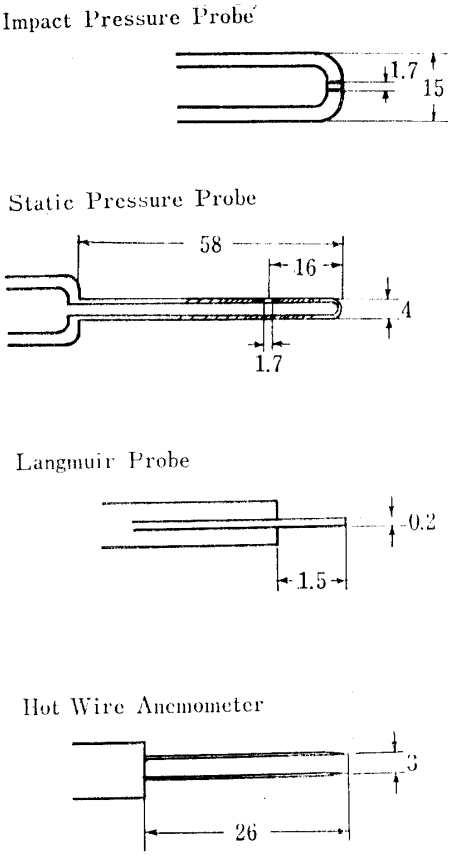

FIG. 4. Probes

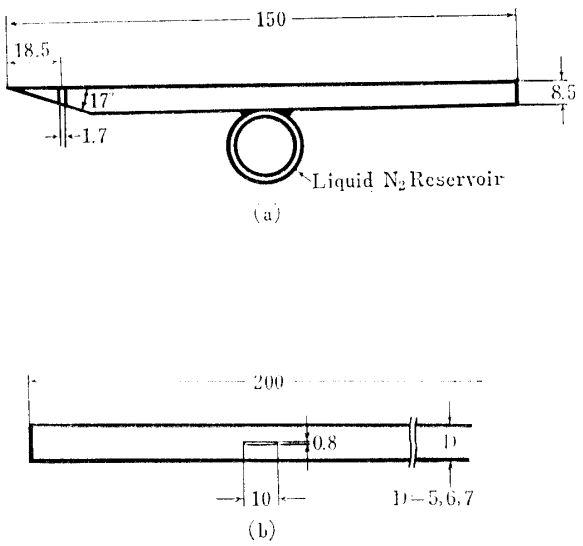

FIG. 5. Models
(a) The sharp leading edge flat plate
(b) The cylinder

plate model was suspended from the top flange of the chamber in the direction parallel to the flow at the position of 5 mm aside from the flow axis, the leading edge of it is 10 mm apart from the nozzle exit. The surface pressures were measured under both the adiabatic and the cold wall conditions. The data were taken for eight cases of the flow rates. The magnitude of the time constant of the surface pressure measuring system is in the same order as that of the pressure probes and no apparent difference due to the surface conditions is observed.

The cylinders are glass or brass tubes with different diameters, and long enough so as to regard the flow field as two-dimensional. The cylinder was placed perpendicular to the flow at the distance of 10 mm downstream of the nozzle exit. The surface pressures of it were measured through a slit of 0.8 mm width and 10 mm length continuously by rotating the model around its axis at a low rate of 19 minutes per one revolution under the adiabatic surface condition, the time constant of this system being about a half as small as that of the pressure probes.

The measured pressures are not necessarily the true impact or the surface pressure unless the molecular mean free path is much smaller than the orifice diameter and/or the gas and the surface are in thermal equilibrium. The orifice effect on the pressure data measured in the rarefied flow has been treated in [27], [42],[50],[51]. Usually the measured pressure data in the rarefied flow are corrected of the viscous and the thermal transpiration effects.

The viscous correction of the measured pressure was performed in this experiment as follows. The surface pressure distribution of the cylinder, P_w, is calculated using the equation of the total pressure in a free molecule flow proposed in [*19*] as

$$P_w = \frac{\rho_\infty U_\infty^2}{2S}\left[\left\{\frac{(2-f_n)}{\sqrt{\pi}}(S\sin\theta)+\frac{f_n}{2}\sqrt{\frac{T_w}{T_\infty}}\right\}e^{-(S\sin\theta)^2}\right.$$
$$+\left\{(2-f_n)\left(S^2\sin^2\theta+\frac{1}{2}\right)+\frac{f_n}{2}\sqrt{\pi}\sqrt{\frac{T_w}{T_\infty}}(S\sin\theta)\right\}$$
$$\left.\times\{1+\mathrm{erf}(S\sin\theta)\}\right],$$

where θ, S, f_n are the angle which the free stream mean velocity vector makes with surface element, the molecule speed ratio and the accommodation coefficient normal to the model surface, respectively. From the ratio of the surface pressure at $\theta=0°(P_{90°})$ to the one at $\theta=90°(P_{0°})$ which is given as

$$\frac{P_{0°}}{P_{90°}}=\left\{\left(\frac{S}{\sqrt{\pi}}+\frac{\sqrt{\Gamma}}{2}\right)e^{-S^2}+\left(S^2+\frac{1+S\sqrt{\pi\Gamma}}{2}\right)(1+\mathrm{erf}\,S)\right\}\Big/\frac{1}{2}(\sqrt{\Gamma}+1),$$

the theoretical relation between $(P_{0°}/P_{90°})$ and S is obtained, which is expressed graphically in Fig. 6, where $\Gamma=1+\frac{\gamma-1}{\gamma}S^2$, and $T_{\infty,0}$ is assumed to be the same as T_w. Using this theoretical curve, the value of S is determined from the measured pressure ratio $(P_{0°}/P_{90°})$, and the free stream static pressure, P_∞, is obtained using the result of Chambré's. The Mach number in the free stream is calculated

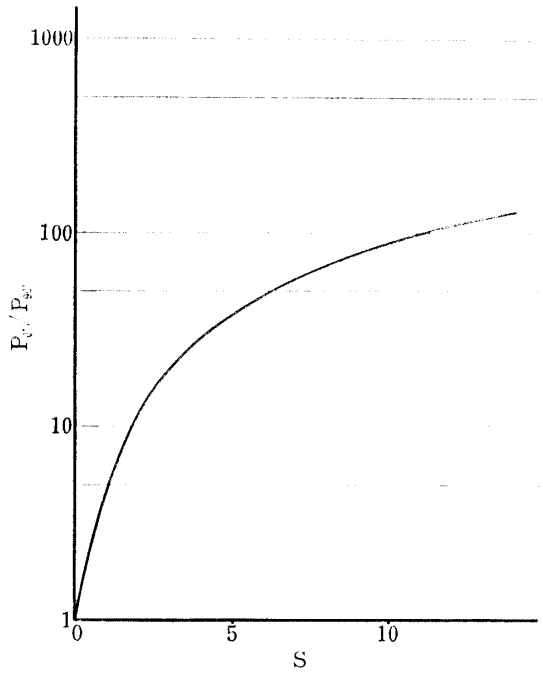

FIG. 6. Theoretical curve relating the surface ratio to the speed ratio

from the value of S determined above using the relation

$$M_\infty = \sqrt{\frac{2}{\gamma}} S ,$$

In this experiment the orifice correction of the surface pressure for thermal transpiration was carried out according to the reference [51]. Potter *et al.* [51] derived the relation between the measured surface pressure, P_j, the true pressure on the surface outside the orifice, $P_{j,or}$, and the heat transfer rate, $\dot{q}$, using the the two-stream Maxwellian velocity distribution as proposed by Liu and Lees [58]. In the limiting case where the mean free path, λ_w, corresponding to the orifice pressure and the wall temperature, T_w, is much larger than the orifice diameter, d, that is $\lambda_w/d \to \infty$, a non-dimensional heat transfer parameter, K_w, is related to the pressure correction factor $(P_j/P_{j,or})_L$ as follows,

$$K_w = \frac{16/15)(2/\pi)^{1/2}[(P_j/P_{j,or})_L - 1]}{(P_j/P_{j,or})_L} ,$$

where the suffix L means the limiting case of $\lambda_w \gg d$, and this parameter, K_w, is defined as

$$K_w = \frac{\dot{q}\,\mathrm{Pr}_w(\gamma-1)}{\gamma P_j(\boldsymbol{R}T_w)^{1/2}} ,$$

where Pr, T_w, are the Prandtl number and the wall temperature, respectively. The mean free path, λ, is calculated by the following relation which is proposed by Patterson [55] as

$$\lambda = \frac{16}{5} \cdot \frac{\mu}{P} \sqrt{\frac{\boldsymbol{R}T_0}{2\pi}} , \qquad (1)$$

where μ is the viscosity and is calculated from the Sutherland's equation for CO_2 gas

$$\mu = \frac{1.554\sqrt{T}}{1 + \dfrac{24.6}{10^{3/T}} \cdot \dfrac{1}{T}} \times 10^{-5} \quad gr/cm \cdot sec .$$

Then Potter defined the normalized pressure correction factor, $\bar{P}$, as

$$\bar{P} = \frac{(P_j/P_{j,or}) - (P_j/P_{j,or})_L}{1 - (P_j/P_{j,or})_L} ,$$

and derived experimentally the relation between this factor and the rlative orifice size and the wall condition for nitrogen and argon gases.

In this experiment, because λ is much larger than the orifice diameter, d, over the whole experimental conditions, one can assume

$$\frac{P_j}{P_\infty} = \sqrt{\frac{T_w}{T_g}} ,$$

where P_w corresponds to $P_{j,or}$ in the prior expressions, and then, (P_j/P_w) is estimated to be 0.58 for the case of $T_g = 300°K$ and $T_w = 77°K$ from the empirical working chart presented in [*51*].

A working chart of the same type based on the experimental results of pressure dependence on the temperatures at the cold and hot ends of a fine tube is presented also in [*50*]. The thermal effects along the wall of the orifice tube were neglected since the orifice length is short in this experiment.

The rarefaction parameter is defined as

$$\bar{V}_{\infty,X} = M_\infty \sqrt{\frac{C_\infty}{\mathrm{Re}_{\infty,X}}} .$$

This parameter mainly has relation with the slip effect which appears near the sharp leading edge of slender bodies when the gas flow becomes rarefied and/or hypersonic [*52*]. The Reynolds number used in the above expression was calculated as

$$\mathrm{Re}_{\infty,X} = \frac{\rho_\infty U_\infty X}{\mu_\infty}$$

where X is the distance along the flow direction from the leading edge to the measuring point, and $\rho_\infty \cdot U_\infty$ is determined as follows under the assumption that a gas is isentropic

$$\rho_\infty U_\infty = \frac{A^*}{A_e} \cdot \rho^* U^* ,$$

where A^* is the throat area and A_e, the effective exit area of the nozzle. Assuming that $T_0 = 300°K$ and the gas is CO_2, then we have

$$\rho_\infty U_\infty = 3.84 \times 10^{-5} \cdot P_0 \cdot \frac{A^*}{A_e} ,$$

where the units of P_0 and A are μHg and cm^2, respectively. The value of C_∞ is assumed to be unity.

The Kundsen Number in this experiment is defined as

$$\mathrm{Kn} = \frac{\lambda_\infty}{D} ,$$

where D is the model diameter, and λ_∞ is the mean free path in the free stream which is calculated by eq.(1).

When the flow becomes rarefied with regard to the orifice diameter, the measured pressures by the impact probe, P_{im}, or by the orifice probe, P_{or}, are influenced by its geometry such as the internal diameter, d, and the length, l, of the probe. The theoretical treatments of the impact and/or the orifice probe in the free molecule flow regime were proposed [*59*],[*63*], and the numerical solution was

presented in [64], which is briefly summarized as follows. With the assumption that the equilibrium Maxwellian velocity distribution superposed on the local mean velocity is realized in the viscinity of the orifice, the balance of the molecules entering to and leaving from the gauge through the orifice per unit time is written for the orifice probe with infinitely large diameter to length ratio as

$$N_s = N_{or} ,$$

where N_s is the number of the entering molecule and N_{or} is the one leaving. After some manipulation, one has

$$\frac{P_{or}}{P_\infty}\sqrt{\frac{T_w}{T_{or}}} = [e^{-S^2} + S\sqrt{\pi}\,(1+\mathrm{erf}\,S)] . \tag{2}$$

For the impact probe, the relation of the same form as eq. (2) is obtained.

$$\frac{P_{im}}{P_\infty}\sqrt{\frac{T_\infty}{T_{im}}} = \frac{W(S, \mathscr{D})}{W(0, \mathscr{D})} ,$$

where $W(S, \mathscr{D})$ is the probability function presented in [64], and $\mathscr{D}$ is the ratio of the diameter to length of the probe. The numerical calculation of (P_{im}/P_{or}) was carried out for speed ratios of zero to 20 and for the ratio of $\mathscr{D}$ from zero to infinity which corresponds to the orifice probe. From this result, it is found that this ratio, P_{im}/P_{or} increases with increasing the value of $1/\mathscr{D}$, and/or S. The same trend as this was confirmed experimentally by Sreekanth [60]. He showed that the measured value of this ratio approaches to the theoretical prediction when the Knudsen number based on the ratio of free stream mean free path to the internal diameter of the probe is more than 10.

The theory of the free molecule impact probe is also presented in [59] in which, after several assumptions, Chambré *et al.* presented a formula which contains, as the parameters, the probe geometry, the free stream Mach number and the ratio of the products of the pressure and the density in the probe and of those in the free stream.

2.3 *Hot Wire*

The hot wire anemometer is a fine platinum wire of 3 mm length and 0.01 mm diameter welded on the top of a pair of stainless steel supports. Conventional hot wire anemometer senses the mass flow rate and the temperature of the flow in a complicated way, but when used in the rarefied hypersonic flow as a free molecule probe, it shows a different performance as described later. This free molecule probe criterion that the mean free path of a flow is sufficiently large compared with the hot wire diameter is realized in this experiment.

The problem of the heat transfer from wires in the rarefied flow is a classical one, and many studies have been reported [20],[32],[43],[61],[62]. When the wire is used as the free molecule probe [20],[43], the heat transfer coefficient, h_w, may be expressed as

$$h_w = Pv_m ag(S)/(2\pi^{3/2}T) , \qquad (3)$$

where v_m, a, are the most probable molecule speed and the accommodation coefficient of the wire surface, respectively, and $g(S)$ is the function of the molecular speed ratio S and is tabulated in the reference [*20*]. In the limiting case of $S \to \infty$, eq. (3) is

$$h_w = 3aR\rho U/\pi ,$$

where U is the mean velocity of the undisturbed flow. The Nusselt number, Nu, in this case is expressed as

$$\mathrm{Nu} = (3aR/\pi C_p)\mathrm{Re}\cdot\mathrm{Pr} , \qquad (4)$$

where C_p, Pr are the specific heat at constant pressure and the Prandtl number, respectively. Eq. (4) indicates that Nusselt number is proportional to Reynolds number and is independent of Mach number when it is sufficiently large.

Hot wire calibration curves which relate the quantity of the heat input to the wire with the wire temperature are shown in Fig. 7. The curves of the three cases which are in vacuum, with the flow and with the model in the flow practically coincide with each other. This indicates that the magnitude of the heat dissipation due to the flow is so small that the conventional analysis as the ordinary hot wire anemometer is useless in order to reduce the property of the flow. Therefore, a new method for estimating the heat transfer due to the flow is proposed here.

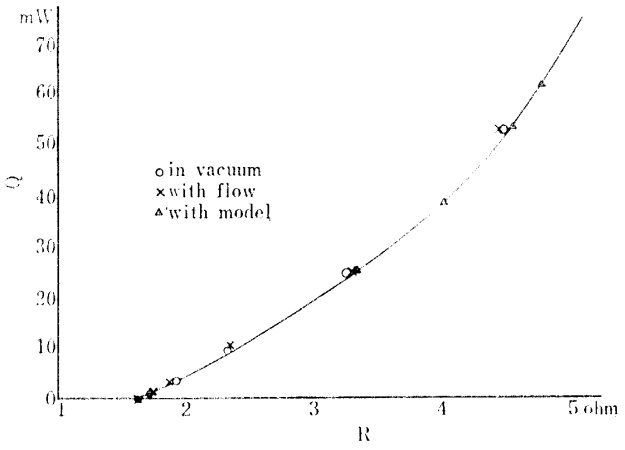

FIG. 7. Hot wire calibration curve

In this experiment the hot wire is operated under a constant current condition. As the heat balance of the hot wire is expressed as follows:
(Joule heating) = *(Radiation loss)* + *(End loss)* + *(Convection loss by flow)*,
the heat loss due to the flow can be determined from the difference between the no-flow and the with-flow conditions. The relation between the heat flux and the wire resistance is shown schematically in enlarged form in Fig. 8, in which Q_0, Q_F, are the characteristic curves for the no-flow and the with-flow conditions, respectively, and Q_s is the supplied heat flux. The difference, ΔQ, between Q_F and

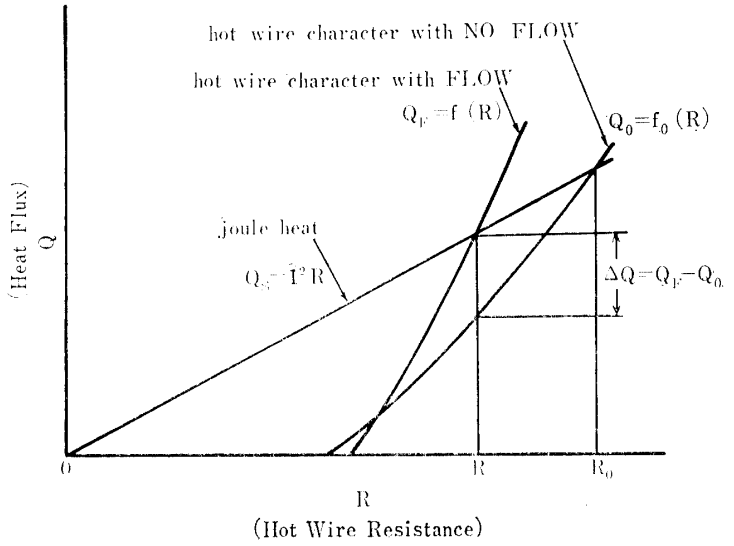

FIG. 8. Explonatory curves for the calculation of the heat transfer rate

Q_0 at a wire resistance, R, corresponds to the dissipating heat flux due to the flow. In this experiment, the quantity of ΔQ is small and the supplied current, I, is constant, therefore

$$\Delta Q = \left(\frac{df_0(R)}{dR}\right)_{R=R_0}(R_0-R) - I^2(R_0-R)$$
$$= \left\{\frac{1}{I}\left(\frac{df_0}{dR}\right)_{R=R_0} - I\right\}\Delta V .$$

Since the voltage difference of the hot wire, ΔV, is measurable with a sufficient accuracy using electronic voltmeter, and the gradient, $(df_0/dR)_{R=R_0}$ is estimated from the hot wire calibration curve, the value of ΔQ is available with enough sensitivity.

The experimental value of Nu is calculated by the following relation

$$\mathrm{Nu} = \frac{\Delta Q}{\pi l k (T_w - T_{we})} ,$$

where l, K, T_w, T_{we}, are the wire length, the thermal conductivity of CO_2 gas, the wire temperature and the equilibrium or no heat transfer temperature of the wire, respectively. If the Nusselt number is assumed to be constant against the wire temperature, the heat loss is linear to the wire temperature, and therefore it is determined from the gradient of the curves relating the heat loss of the wire to the wire temperature (or the wire resistance). The typical relations of the heat loss to the wire resistance are shown in Fig. 9. The experimental values of Nu are shown in Fig. 10, in which the free molecule theory and the experimental values of Dewey *et al.*'s [20],[43] are also indicated. The result of this experiment qualitatively agrees with the free molecule probe theory. In the range of this experimental condition, the heat loss by the rarefied flow is so small compared with that of the radiation or the conduction that the measurement of the heat dissipation is

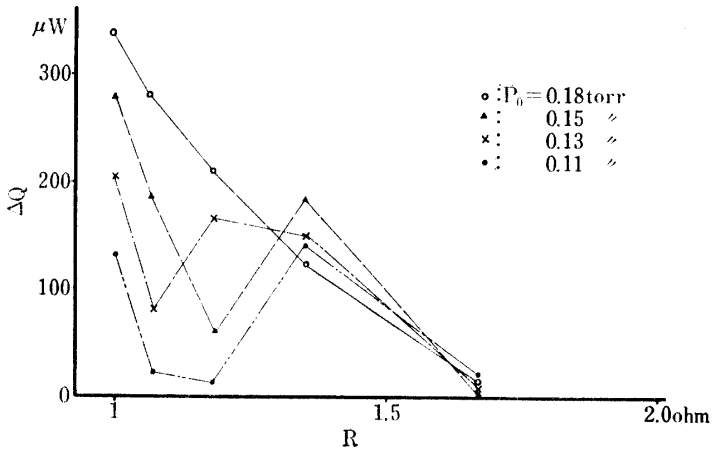

FIG. 9. The heat transfer rate due to the flow with the relation to wire resistance

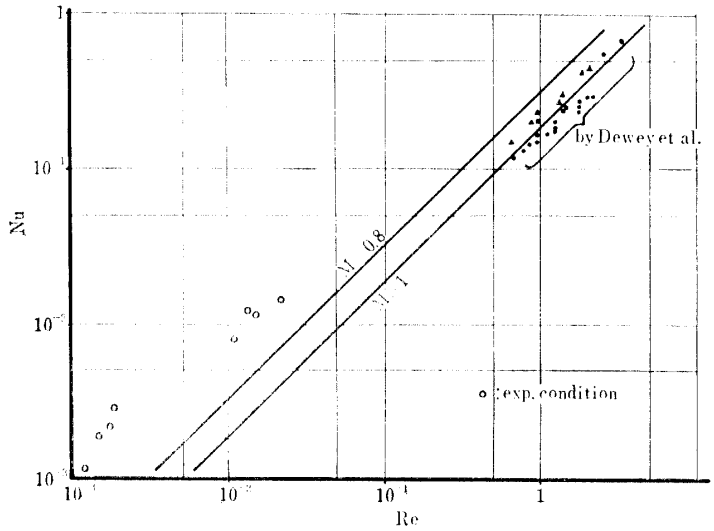

FIG. 10. The Nusselt number with the relation to the Reynolds number

difficult and the measured values are rather scattered, but the correlation of Nu with Re is clearly presented in this result.

Fig. 11 shows the change of the heat transfer due to the flow angles and the mass flow rates, in which the symbols, $\perp$, // mean the cross and the parallel directions of the wire to the flow, respectively. The heat transfer change of the wire is low when a mass flow rate is small, but as the mass flow rate increases, it becomes higher. The angle dependence of the heat transfer rate is clearly seen in the figure. Quantity of dissipating heat flux due to the mean flow to the wire is approximately constant against the change of the wire temperature. It means that correction of the radiation loss or the end loss is not important when the wire temperature is within this range.

The hot wire anemometer serves as a free molecule probe in the flow field. The wire calibration was carried out whenever a wire was replaced by the new one, for each wire has a different characteristics of the heat dissipation. Since a new

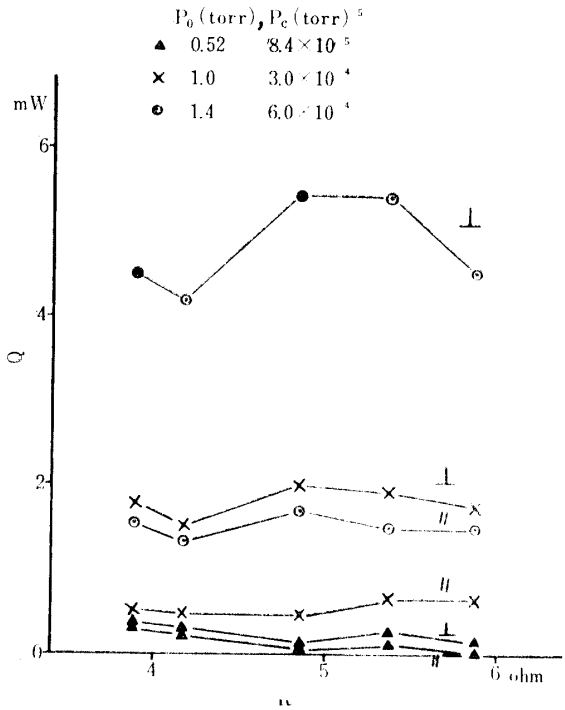

FIG. 11. Hot wire sensitivity to the flow direction

wire sometimes shows unstable nature, a careful ageing by exposing it in the vacuum with a modelate heat supply is necessary. A wire may endure the heating current as high as 150 to 200 mA, but in the actual measurement it is maintained about 120 mA in order to avoid burn-out and to keep the effects of the radiation and the end loss of the wire within a tolerable range. The hot wire probe can be traversed in the flow field and can approach to the model surface as close as 1 mm. The time constant of a hot wire is small enough comparing to the traversing speed, therefore the continuous data recording is available at the traversing speed of 1 mm per second.

2.4 *Langmuir Probe*

Langmuir probe was used for density measurement of the flow field using the ion current characteristics collected to the probe. Usefulness of the Langmuir probe in the molecule flow region was reported by Sonin [*53*], who performed experiments to determine the behavior of small cylindrical Langmuir probe in high speed rarefied flows, and obtained the electron and the ion number densities and the electron temperature using the Laframboise's theoretical results [*54*]. When the probe is applied a negative potential, V, the absolute magnitude of the ion and the electron current densities at the probe surface are expressed as

$$j_i = eN_i\left(\frac{kT_e}{2\pi m_i}\right)^{1/2} \mathrm{I}_i(\chi_p,\ T_i/T_e,\ R_L/\lambda_D) \tag{5}$$

$$j_e = eN_e\left(\frac{kT_e}{2\pi m_e}\right)^{1/2} \exp(\chi_p) \tag{6}$$

where

$$\chi_p = eV/kT_e ,$$

and I_i is the non-dimensionalized ion current density, the magnitude of which is found from the Laframboise's theory as the function of χ_p, T_i/T_e and R_L/λ_D. Differentiating the equation (6), one has

$$\frac{1}{j_e}\cdot\frac{dj_e}{dV} = \frac{e}{kT_e} ,$$

and after some manipulation, the following relation is given

$$\frac{kT_e}{e} = \frac{j_i}{\dfrac{dj}{dV} - \left|\dfrac{dj_i}{dV}\right|}\Bigg|_{V=V_f} ,$$

where j is the total current to the probe and is expressed as

$$j = j_e - j_i$$

Based on this relation, the electron temperature is determined graphically on the characteristic of the probe, as shown in Fig. 12 (a). Now, a parameter $\beta = (R_L/\lambda_D)^2 I_i$ is introduced, and using the value of T_e determined by the above process and the experimental value of j_i, this parameter is calculated from

$$\beta = \frac{R_L^2}{\varepsilon_0}\left(\frac{2m_i}{e}\right)^{1/2}\cdot\frac{j_i}{(kT_e/e)^{3/2}} ,$$

where j_i is the probe current at a sufficiently negative potential that j_e is negligibly small. Using the value of β thus determined and the theoretical relation shown in Fig. 2-12 (b), the value of I_i is obtained, and finally the values of N_i and N_e are calculated from the equations (5) and (6).

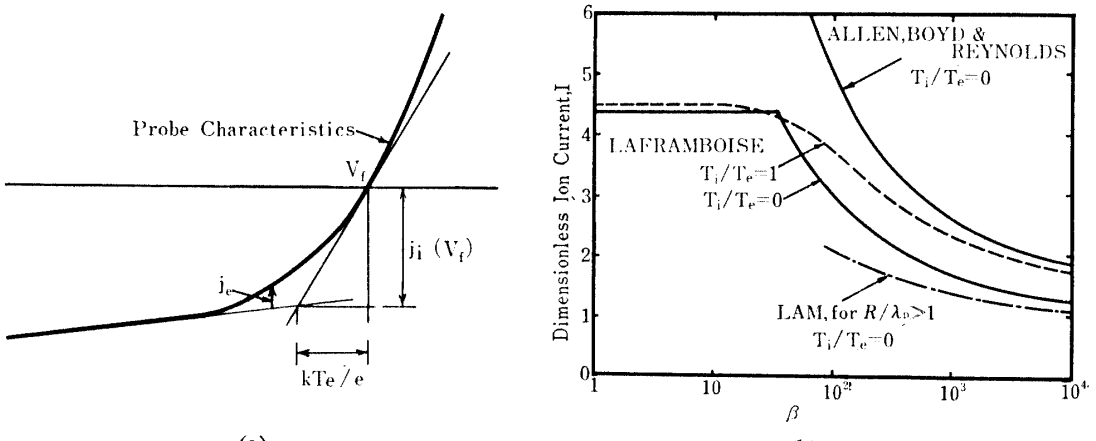

(a) (b)

FIG. 12. Langmuir probe performance (from reference [53])
(a) The ion current region of the probe characteristics
(b) Ion current at a dimensionless probe potential of -15

In this experiment the distribution of the ion current was surveyed by the Langmuir probe at a fixed negative potential of $-50\ V$. The Langmuir probe is made of tungsten wire of 0.1 mm diameter enclosed in a fine glass tube of 1 mm in external diameter. In a weakly ionized gas flow as this, the density of charged particles is considered to be proportional to the one of neutral particles. The rough estimation of the Debye shealding length results in a length of an order of the millimeter in the smallest flow rate, so that very close to the cylinder surface, Langmuir probe survey may fail.

The micro-wave discharge in the plenum chamber is used in the Langmuir probe measurement, which is maintained only in a limited range of the plenum chamber pressure [56]. This method is applied to the flow with the smaller flow rate, while hot wire method is useful in the larger condition.

2.5 *Freeze up Method*

To visualize the flow field, "freeze up method" for carbon dioxide is devised which in principle is analogeous to cryopumping, and is useful in a rarefied flow region where schlieren technique or other conventional method is useless. Flow particles colliding with a cold plate located in the flow lose their energy and most of them are captured and condensed on the surface. The amount of the condensed particles is proportional to the product of the local number density of the flow and the particle mean velocity. Furthermore, as the particle mean velocity is almost uniform in a fully rarefied flow, the general view of the density distribution is known from the distribution of the accumulation of the condensed particles on the plate. The thickness can be read by the methods of polarimetry or interferometry or others, but the simplest method is direct observation under tangential skew illumination. The visualization of a flow field around a cylinder model is possible when the model is attached normal to the plate. From these photographs, the flow expansion into the vacuum, the shock formation and the wake pattern of a cylinder were visualized [57].

2.6 *Flow Field Survey*

As the preliminary step of the experiment using the flat plate or the cylinder, the flow field condition of this tunnel was surveyed by several probes and by freeze up method.

The static or the impact pressures in the flow field were measured by the pressure probe, which were observed on the chart record of the pressure reading. The time constant of the pressure measuring system varies from a few seconds to 2 minutes at most and becomes larger as the flow rate decreases. These flow field maps are shown in Fig. 13(a)(b) which were derived from the impact pressure probe survey, and in Fig. 14(a)(b) those derived from the static pressure probe survey. With these maps of pressure distribution the test section of the tunnel is found to have a wide uniform flow region.

Fig. 15 shows a result of the hot wire survey. The figures in the map indicate the difference of heat transfer rate from the one at the nozzle exit center.

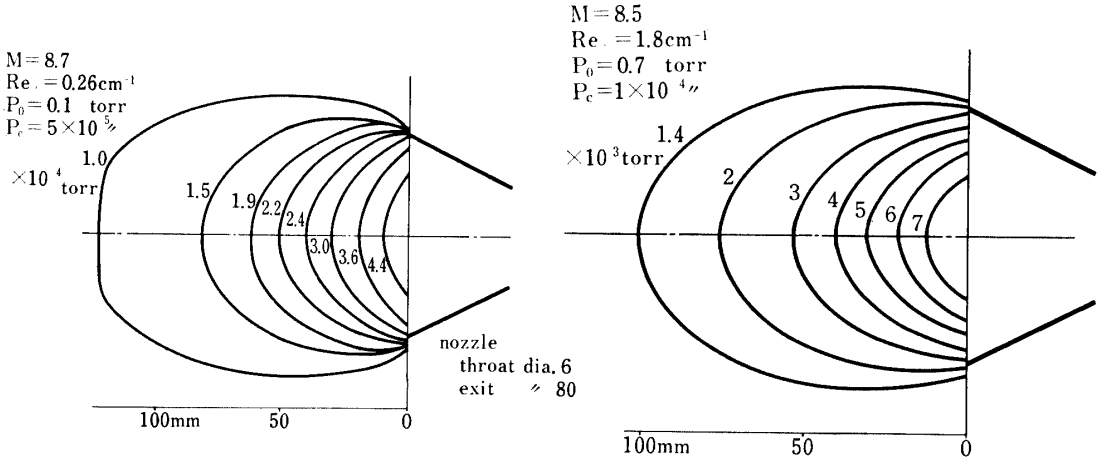

FIG. 13. Pressure distribution in the flow field (by the impact pressure probe)

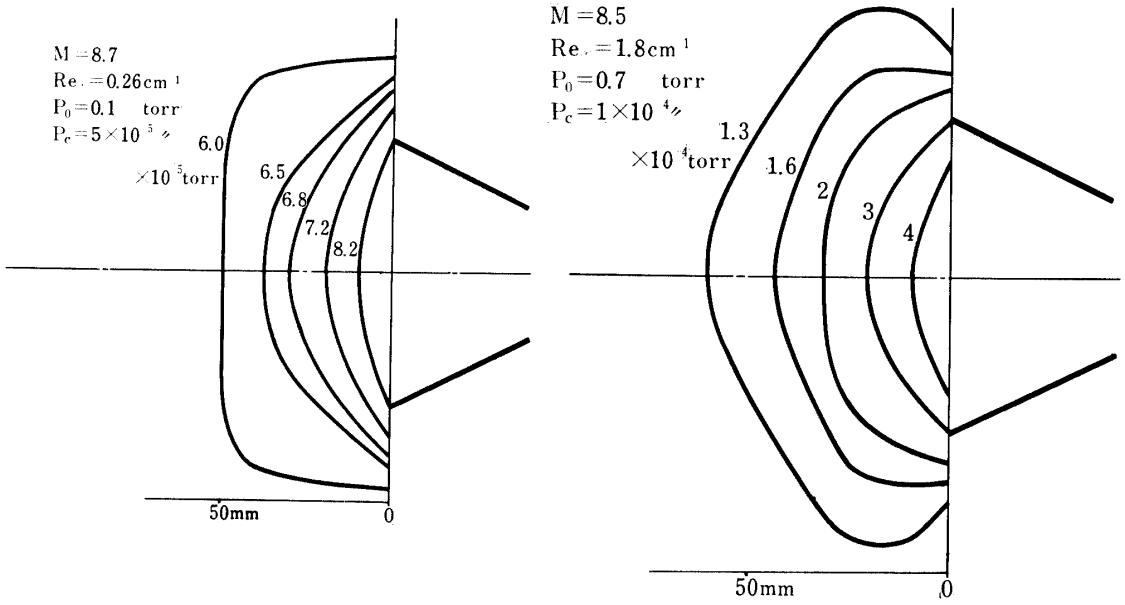

FIG. 14. Pressure distribution in the flow field (by the static pressure probe)

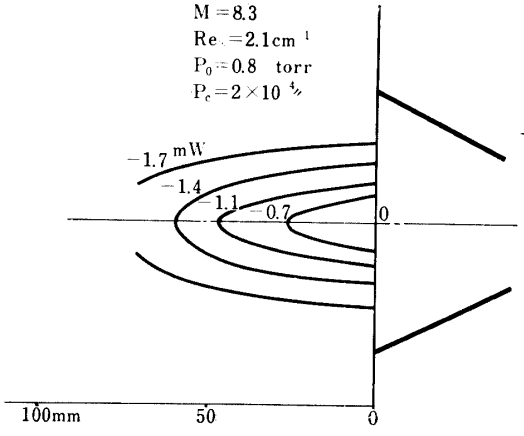

FIG. 15. Heat transfer rate due to the flow (by hot wire anemometer)

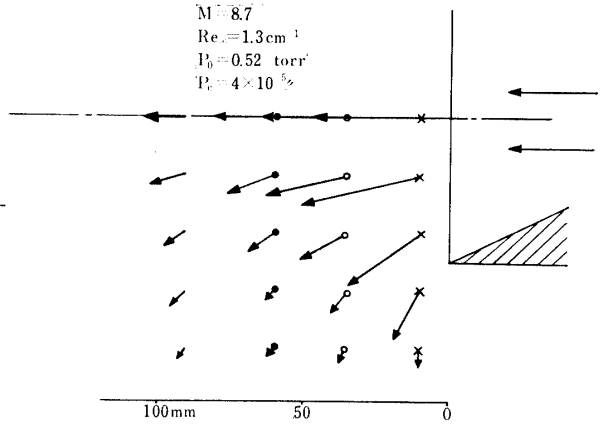

FIG. 16. The distribution of the free stream velocity vectors (by the hot wire anemometer)

Fig. 16 shows a flow direction map of a nozzle flow reduced from the hot wire survey.

The typical photograph of the flow field by freeze up method is shown in Fig. 17.

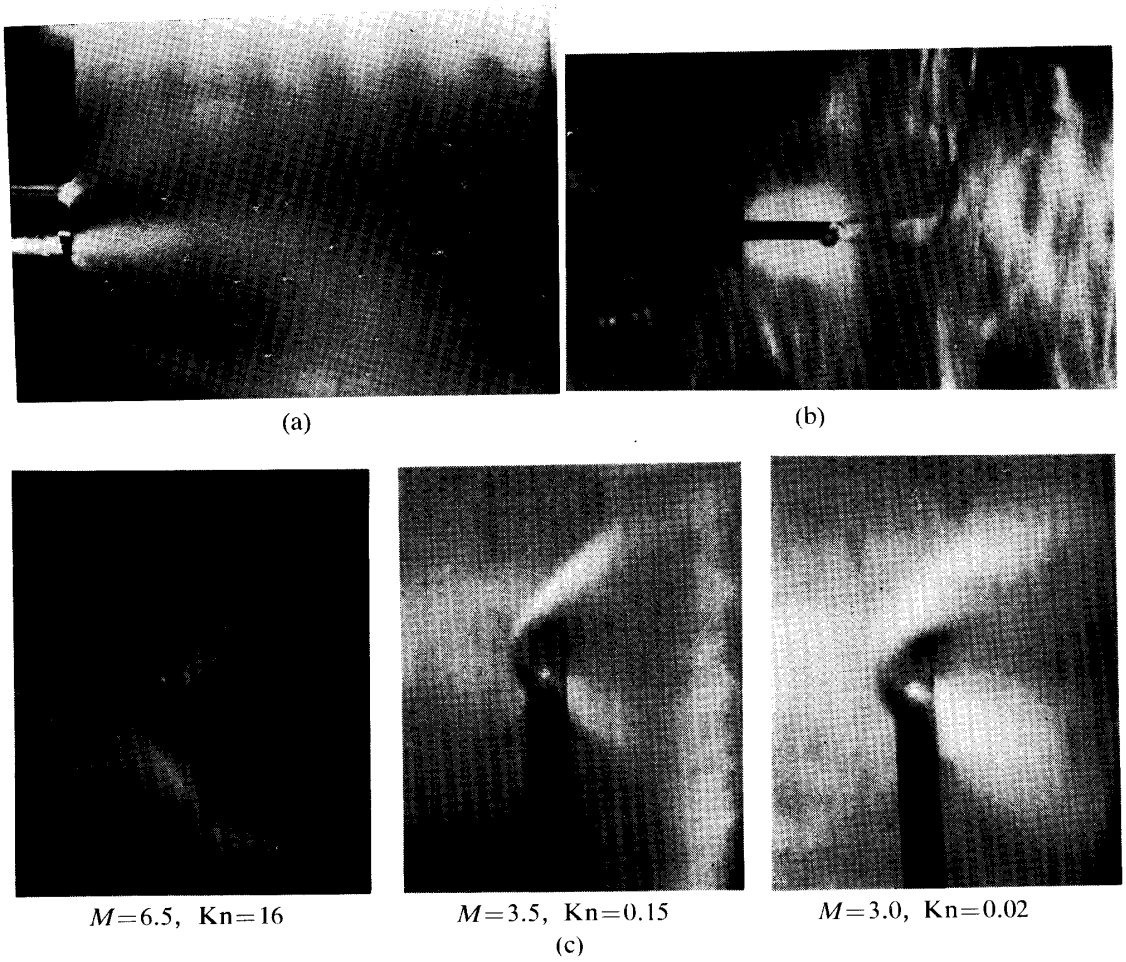

FIG. 17. Photographs by means of freeze up method
(a) View of the free stream in the flow field
$M=7$, $P_0/P_\infty=6.7\times10^4$
(b) Flow pattern around the cylinder
$M=4.0$, Kn$=54$
(c) Flow pattern around the cylinder

3. Results and Discussion

3.1 *Sharp Leading Edge Flat Plate*

The sharp leading edge problem is to understand gasdynamical phenomena observable between a free stream and a disturbance flow which necessarily appears near the leading edge region. Recently this problem has been a most favorable object to see the transition from microscopic kinetic to macroscopic continuum behaviors. In the analytical treatments of the sharp leading edge problem, the flow fields are categorized usually into the several regions [*1*],[*35*], for convenience.

Roughly, far downstream from the leading edge is a weak interaction region and in upstream direction the flow field is successively divided into a strong interaction region, a merged layer region and a free molecule flow region toward the leading edge. Here the merged layer region corresponds to a so-called transition region, though the latter term is often used in a wider sense. In the merged layer region the shock layer merges so completely into the boundary layer that no discrete and thin shock which is seen in the strong interaction region or the weak interaction region is observable any more In this region the density ratio across the shock layer decreases toward the leading edge even though the shock angle increases. Therefore the transport phenomena through the shock layer become important. On the other hand, the slip effects on the surface can no longer be neglected and

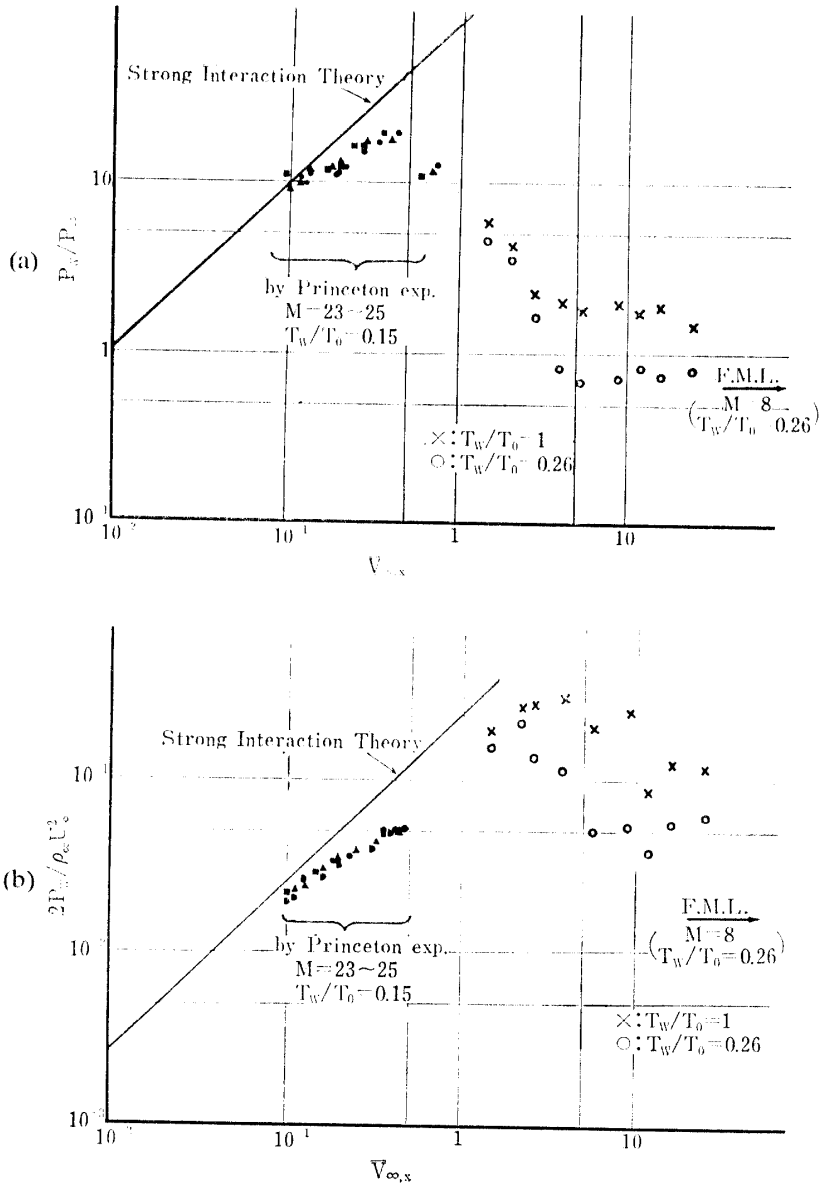

FIG. 18. Normalized surface pressure distribution with the relation to the rarefaction parameter

cause to depart the values of the surface pressure, the heat transfer or the skin friction from the prediction by the strong interaction theory. This departure begins at a certain constant value of the rarefaction parameter, and according to the recent experimental results [32],[33],[35], this is about 0.25, though this figure shows rather wide scattering by the investigators. However, there are many questions left unknown concerned with the merged layer region, the experimental results and the analytical predictions appeared in the publications, therefore, are not consistent with each other.

The measured surface pressures on the plate are shown in Fig. 18(a), (b), with the relation to the rarefaction parameter. The data on the right side are the present ones, and those on the left side are by Harbour *et al.* [36]. The measured pressures cover the wide range of the rarefaction parameter, $\bar{V}_{\infty,x}$, from unity to 20, which well extends beyond the past experimental conditions. The measured values are between the prediction by the strong interaction theory and the free molecule limit, which shows that the present experimental conditions lie in the merged layer region. Though the data are rather scattered, it is noted that the surface pressure with the cold wall is lower and nearer to the free molecule limit than that of the adiabatic condition. This can be explained as follows; as the temperature difference between the surface and the incident particles colliding with it is large in the case of the cold wall condition, the particles lose large part of their thermal energy to the surface. The wall surface emits some part of the particles except those captured on the wall as low energy particles, so that the layer of the low energy particles is formed in the viscinity of the surface to result in the reduction of the surface pressure. The value of P_w/P_∞ has a trend to approach monotonically to the free molecule limit with the increase of $\bar{V}_{\infty,x}$. Especially, in the range of $\bar{V}_{\infty,x}$ larger than 5 with cold wall condition, this value almost equals to the free molecule limit, which may indicate the existence of a free molecule flow in the leading edge region. Here the values of the free molecule limit in Fig. 3-1(a), (b) were calculated by the relations proposed in references [15] and [19] as

$$\frac{P_w}{P_\infty}=\frac{1}{2}\left\{1+M_\infty\left[\frac{1}{2}(\gamma-1)\left(\frac{T_w}{T_0}\right)\right]\right\}$$

and

$$\frac{P_w}{\frac{1}{2}\rho_\infty U_\infty^2}=\frac{1}{\gamma M_\infty^2}\left(1+\sqrt{\frac{T_w}{T_0}}\right),$$

where the value of γ was assumed to be 1.4 in the calculation. The constant plateau of the surface pressure which was predicted in the merged layer region by the analysis [5], however, was not seen in this experiment. As to the existence of the free molecule flow near the leading edge, much discussion has been made: Nagamatsu *et al.* [22] showed the existence of a plateau and Burke [26] showed a gentle slope rather than a plateau, and Chuan [24] did not observe its existence. Also it must be taken into account that near the leading edge a measured surface pressure is considerably influenced by the experimental conditions such as configula-

tion, magnitude, location, surface temperature of orifice, or time constant of the measuring system and so on [*35*]. Furthermore, it is worthwhile to consider again whether the correlation of a surface pressure to the rarefaction parameter has a sound physical basis, or whether there actually exists a free molecule flow region near the leading edge.

In Fig. 19 is shown the ratio of the thickness to the shock height reduced from the hot wire survey. This indicates the rate of the shock thickening in the merged layer and serves as the extension of the data by Becker *et al.* [*33*]. The process of the shock thickening can be seen over the whole range of the rarefaction parameter and is almost independent of the surface temperature.

The characterisitc height Y_B which may represent the shock location is shown in Fig. 20, which is obtained from the hot wire survey profiles. The shock loca-

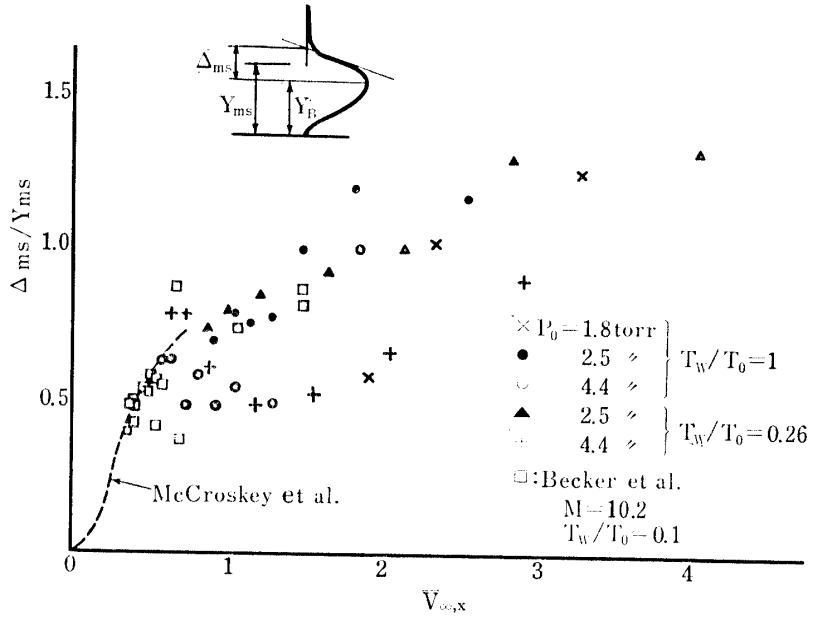

FIG. 19. Ratio of the thickness to the height of the shock layer

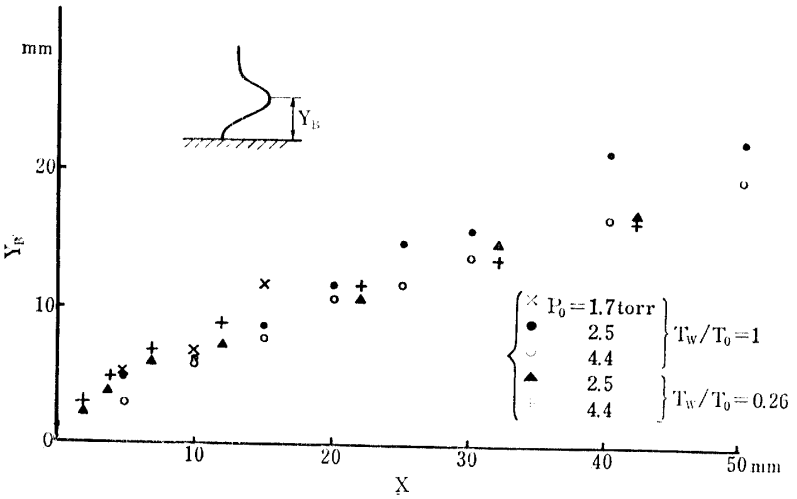

FIG. 20. Characteristic height of the shock layer with the relation to the distance from the leading edge

tion is also nearly independent of the surface temperature. The same trend is observed in the Langmuir probe survey. This result may seem to be surprising on the point of view of the common thought that the shock layer comes close to the surface when its temperature becomes lower than that of the flow. However, according to the experimental results in Fig. 21(a), (b), which give the shock structure in the merged region, the surface temperature effect on the flow field is restricted in the viscinity of the surface.

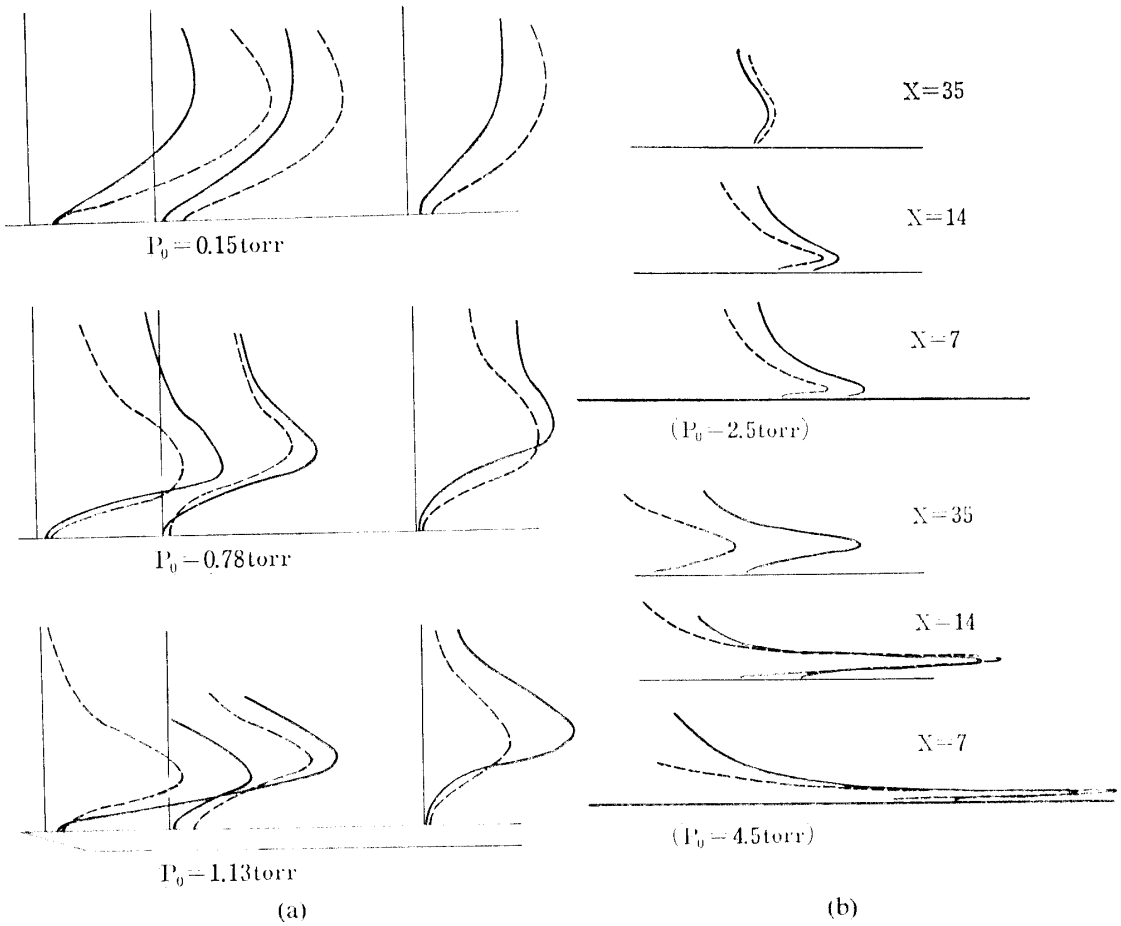

FIG. 21. Profiles by the probe surveies (The solid curve shows the adiabatic wall condition $T_w/T_0=1$ and the dotted one the cold wall condition $T_w/T_0=0.26$.)
(a) Profiles by Langmuir probe survey
(b) Profiles by hot wire survey

Fig. 22 shows the maximum density in the shock layer reduced from the Langmuir probe survey profiles. The data on the left side show those of [36] and the Rankine-Hugoniot relation. The measured values are almost independent of rarefaction parameter, and smaller than that of the Rankine-Hugoniot relation. The maximum density is not influenced by the surface temperature in the large rarefaction parameter range as this. From these results of Figs. 19, 20, 21, 22, it is clear that the flow fields are almost independent of the surface temperature in the hypersonic rarefied flow, except the region very close to the surface.

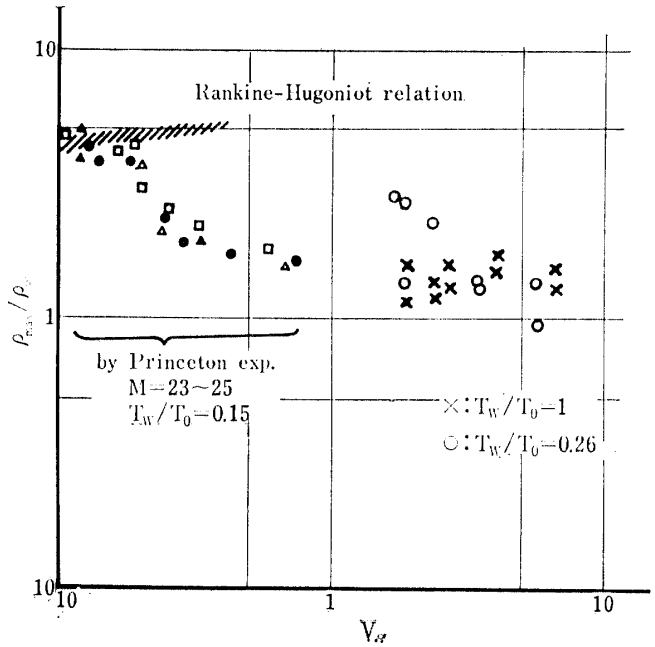

FIG. 22. Maximum density in the shock layer (reduced from the Langmuir probe survey)

Fig. 23 (a), (b), (c) show typical maps of the flow field reduced from the hot wire dissipating into the flow in micro watt (μW). From this series of maps, the process of the shock formation can be seen; the flow disturbances firstly generated at the leading edge grow and develop to downward with the increasing Reynolds number, and finally make up thick and weak shock layer.

3.2 *Circular Cylinder*

Fig. 24 (a), (b), (c) show representative flow field maps around a circular cylinder reduced from the Langmuir probe survey profiles using the weakly ionized argon gas, the figures indicate the density ratio in the flow field, ρ/ρ_∞, in per centage(%).

Fig. 25 (a), (b) are also typical flow field maps reduced by the hot wire survey profiles, the figures indicate the dissipating heat rates of a wire in micro watt. With these maps of several flow field conditions, the birth and growth of a bow wave around a cylinder can be thoroughly seen. In the case of large Knudsen number, no distinct density condensation is observed in front of the cylinder, but with the decrease of Kn there appears an obvious density rise at the shoulder of the cylinder as seen in Fig 24 (c) which is called "shoulder wave". This "shoulder wave" grows with the successive decrease of Kn, and when Kn reduces to unity or below, two shoulder waves from both sides move forward to form a weak but distinct bow wave, the stand-off distance of which is larger than that predicted by the continuum theory. The location of this wave moves toward the cylinder as Kn goes to zero. On the other hand, the behavior of the wake is quite similar to that of the free molecule flow when Kn is large, and agree well with that of the viscous layer theory when Kn is small. These qualitative phenomena are found

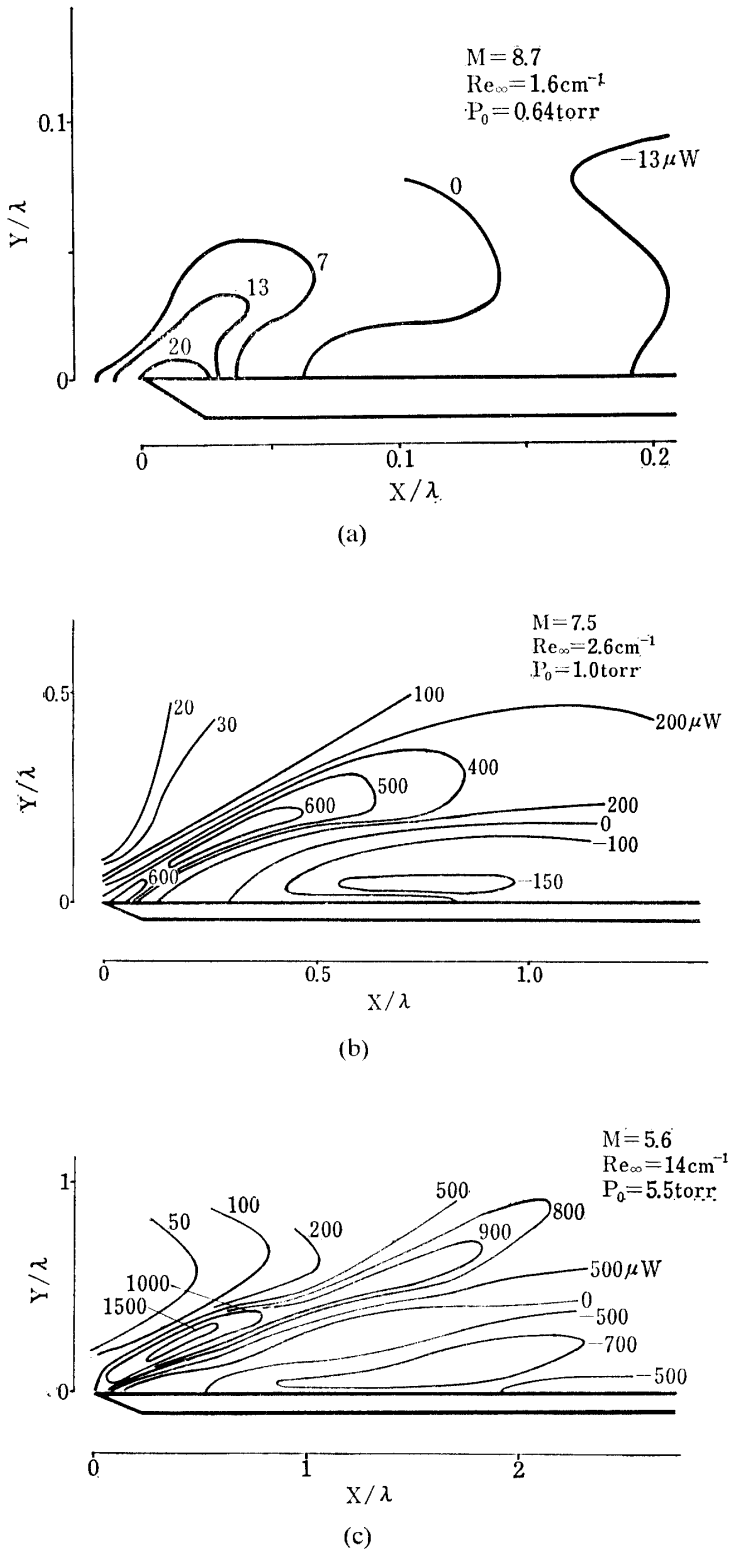

FIG. 23. Flow pattern past the sharp leading edge flat plate (reduced from the hot wire survey)

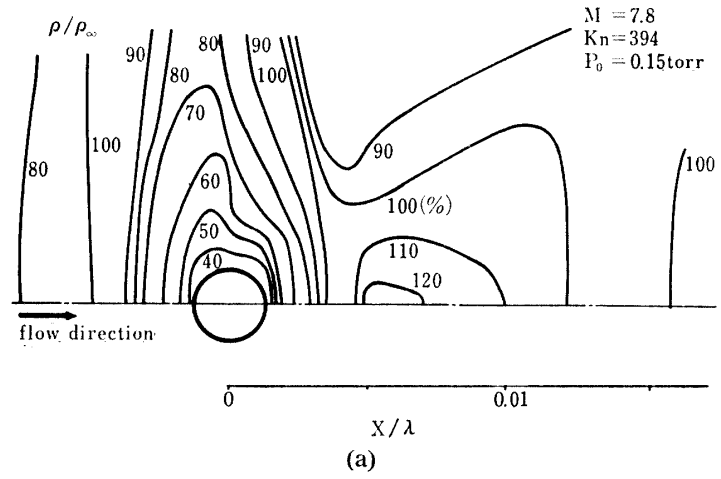

(a)

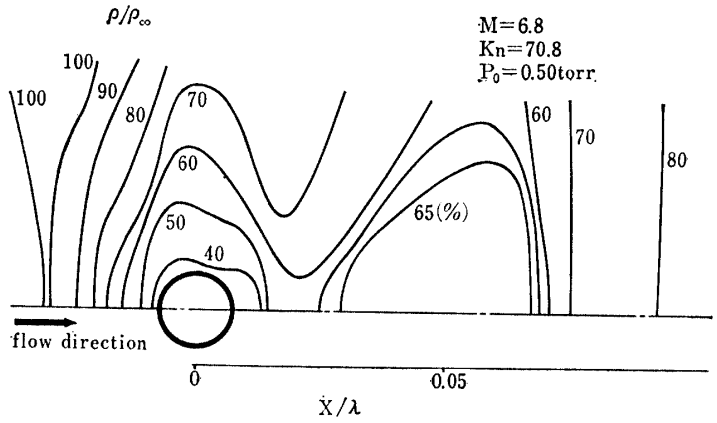

(b)

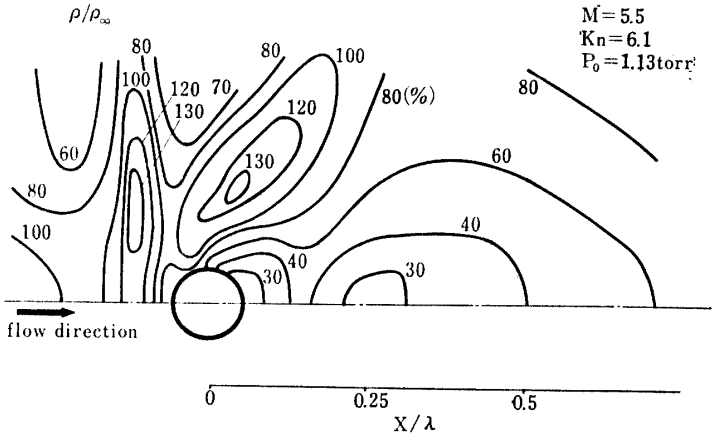

(c)

FIG. 24. Flow pattern around the cylinder (reduced from the Langmuir probe survey)

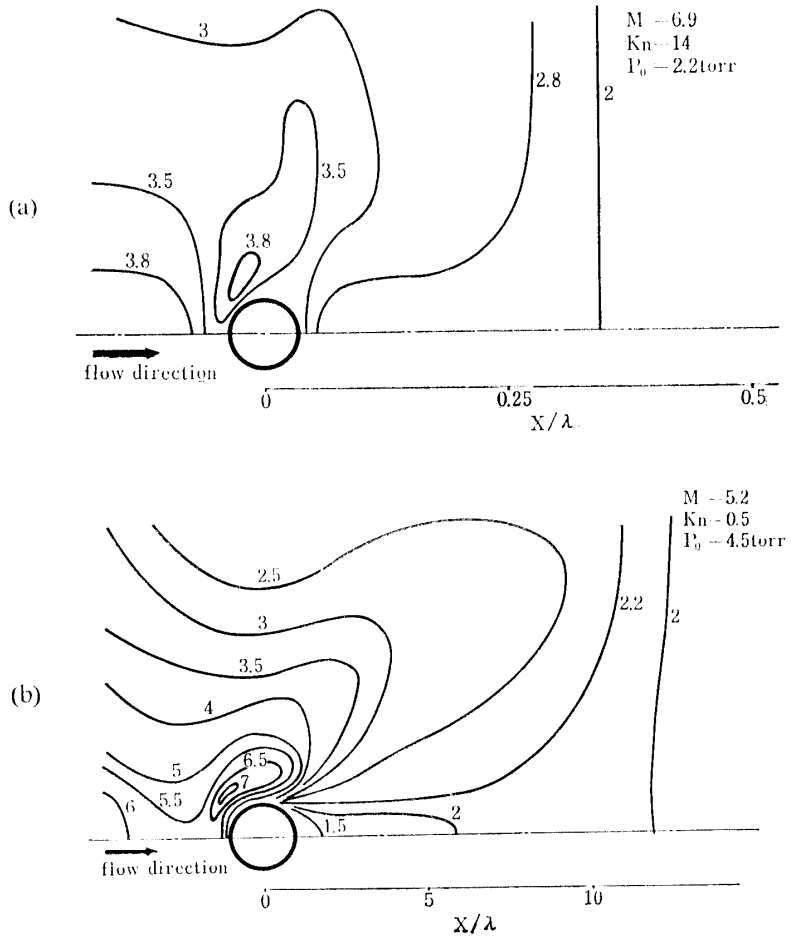

FIG. 25. Flow pattern around the cylinder (reduced from the hot wire survey)

on the photographs of the freeze up method. The typical photographs of the flow pattern around the cylinder are shown in Fig. 17 (a), (b). The density distributions along the flow axis of the cylinder are illustrated in Fig. 26 (a), (b), (c). It is confirmed from these data that in the case of larger Kn no density rise is found in the front portion and the wake pattern is similar to that of a free molecule flow. The fact that the density distribution drops lower than the free stream value in the viscinity of the cylinder may be influenced by the sheath effect of the cylinder. Because the Debye shealding length is small, this sheath effect is restricted only the close region to the cylinder.

The normalized surface pressure distributions around the cylinder are shown in Fig. 27. The normalization of the surface pressure is carried out by the impact pressure and the base pressure, i.e.

$$\frac{P_w - P_{180°}}{P_{0°}},$$

where $P_{0°}$, $P_{180°}$ are the impact and the base pressure, respectively. In the numerator of the normalized pressure above, the base pressure is subtracted from the surface pressure so that the differences between the real pressure and the measured

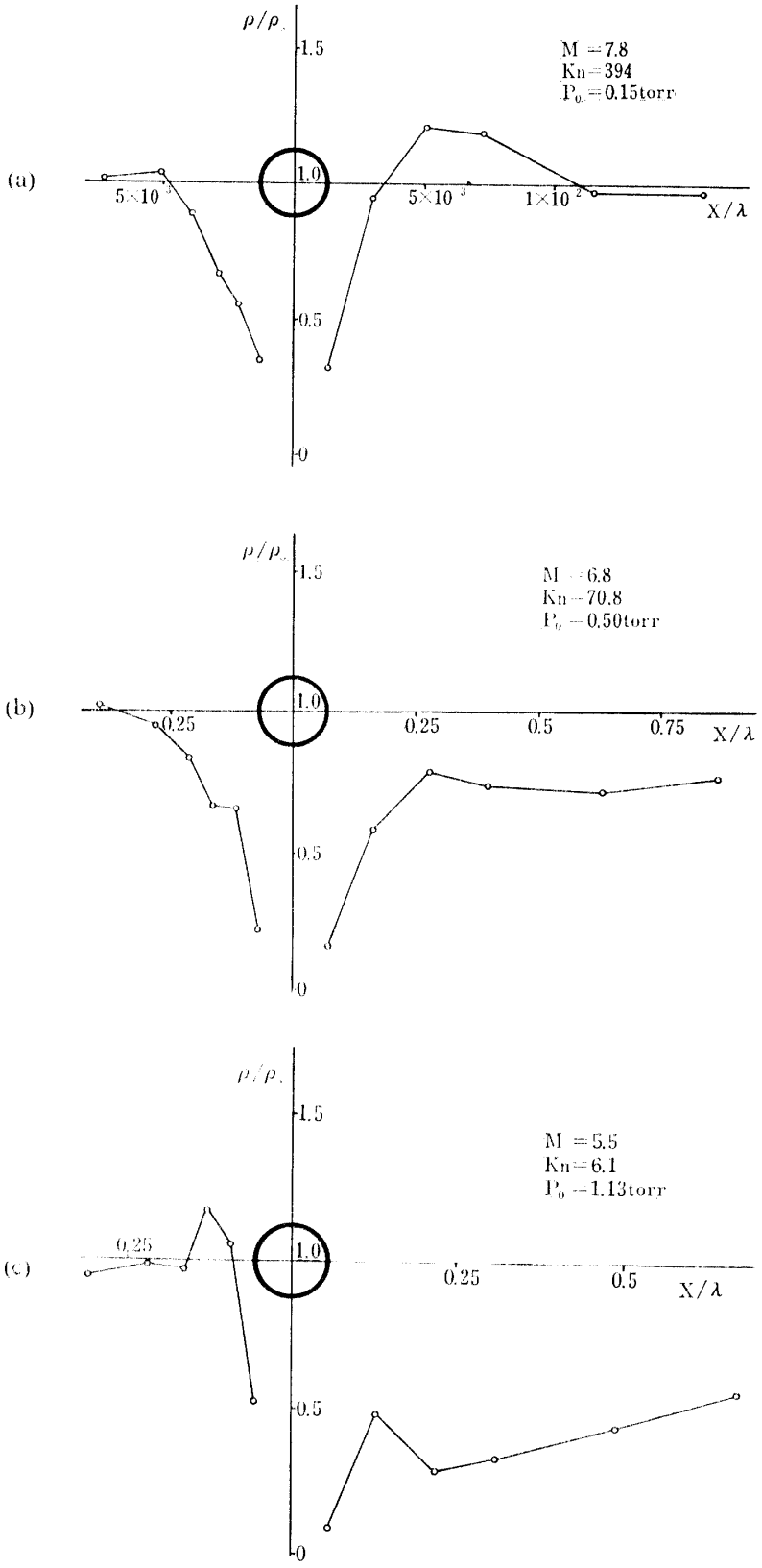

Fig. 26. Density distribution around the cylinder along the flow axis

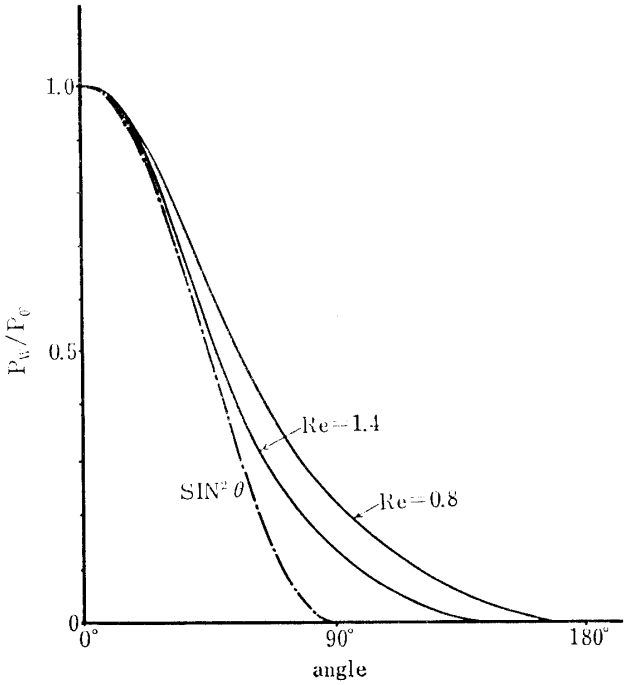

FIG. 27. Normalized surface pressure distribution around the cylinder

one may cancel each other. No clear separation point is distinguishable, and in the rear portion of the cylinder the surface pressures become zero over more than 150°. The pressure recovery is not found in the wake just as in the case of a free molecule flow. The distributions in the front portion agree well with that of the Newtonian theory. When the Reynolds number decreases, the distributions become gentle, that is, the spatial differences of the surface pressures decrease. This trend is in contrast to the result of [47]. Zapata *et al.* [47] found a very significant drop in the base pressure at the low free stream Reynolds numbers of 1200 to 3000, which are considerably higher than this experiment.

4. CONCLUSION

The rarefield gas flows with large rarefaction parameters up to 20 for the flat plate and with Knudsen numbers up to 400 for the cylinder are obtained using the wind tunnel with cryo-pumping capability. The detailed measurements of rarefied flow field were carried out using the several methods. The complete survey of the flow field was made.

The experimental study of the flow field around the flat plate with the sharp leading edge shows that measured values of the surface pressure are between those predicted by the strong interaction theory and by the free molecule theory, and that this values strongly depend on the wall temperature. The shock layer thickness and the location of it are independent of the wall temperature. The density rise at the shock layer is lower than the one predicted by the Rankine-Hugoniot relation and is almost independent of the rarefaction parameter.

The flow character around the cylinder with large Knudsen number is close to the one predicted by the free molecule theory. As the Knudsen number decreases, the density concentration region called "shoulder wave" appears in the neighbourhood of the shoulder at the Knudsen number of about unity. With the decreasing Knudsen number, this soulder wave grows and moves to the forward portion of the cylinder. And finally the bow wave is formed. The wake of the cylinder shows the character predicted by the viscous flow theory for low Reynolds number flow.

Department of Aerodynamics
Institute of Space and Aeronautical Science
University of Tokyo, Tokyo
March 25, 1969

References

[1] S. A. Schaaf: "Recent Progress in Rarefied Gasdynamics" ARS Jour. 30, 443–447, May (1960).
[2] J. L. Potter: "The Transitional Rarefied-Flow Regime" Rarefied Gas Dynamics suppl. 4. vol. II. 881–937 (1967).
[3] J. A. Clark: "Theory and Fundamental Research in Heat Transfer", Oxford and Pergamon Press, 33–60 (1963).
[4] H. Oguchi: "The Sharp Leading Edge Problem in Hypersonic Flow", Rarefied Gas Dynamics suppl. 1, 501–524 (1961).
[5] H. Oguchi: "Leading Edge Slip Effects in Rarefied Hypersonic Flow", Rarefied Gas Dynamics suppl. 2, vol. II, 181–193 (1963).
[6] R. F. Probstein and Y. S. Pan: "Shock Structure and the Leading Edge Problem", Rarefied Gas Dynamics suppl. 2, vol. II, 194–211 (1963).
[7] S. H. Maslen: "Second-Order Effects in Laminar Boundary Layers", AIAA Jour. vol. I, No. 1, 33–40 (1963).
[8] J. A. Laurmann "Structure of the Boundary Layer at the Leading Edge: of a Flat Plate in Hypersonic Slip Flow", AIAA Jour. vol. 2, No. 9, 1655–1657 (1964).
[9] J. A. Laurmann: "Simplified Equations for Hypersonic Viscous Flow Past Slender Bodies", AIAA Jour. vol. 4, No. 3, 568–570 (1966).
[10] G. R. Inger: "Nonequilibrium Hypersonic Flat-Plate Boundary Layer Flow with a Strong Induced Pressure Field", AIAA Jour. vol. 2, No. 3, 452–460 (1964).
[11] A. F. Charwat: "Molecular Flow Study of the Hypersonic Sharp Leading Edge Interaction", Rarefied Gas Dynamics suppl. 1, 553–578 (1961).
[12] G. N. Patterson: "A Synthetic View of the Mechanics of Rarefied Gases", AIAA Jour. vol. 3, No. 4, 577–590 (1965).
[13] G. A. Bird: "Aerodynaic Properties of Some Simple Bodies in the Hypersonic Transition Regime", AIAA Jour. vol. 4, 55–60 (1960).
[14] H. Oguchi: "Shock Wave and Viscous Layer Structure in a Rarefied Hypersonic Flow Near the Leading Edge of a Sharp Flat Plate", ISAS Rept. No. 418 (vol. 32, No. 11) (1967).
[15] M. L. Shorenstein and R. F. Probstein: "The Hypersonic Leading-Edge Problem", AIAA Jour. vol. 6, No. 10, 1898–1906 (1968).
[16] S. Rudman and S. G. Rubin: "Hypersonic Viscous Flow over Slender Bodies with Sharp Leading Edges", AIAA Jour. vol. 6 No. 10, 1883–1890 (1968).
[17] W. B. Bush: "On the Newtonian Hypersonic Strong-Interaction Theory for Flow Past a Flat Plate", Rarefied Gas Dynamics suppl. 4, vol. II, 939–954 (1967).
[18] J. A. Laurmann: "Preliminary Results of a New Formulation of the Hypersonic

Leading Edge Flow Problem", Rarefied Gas Dynamics suppl. 4, vol. II, 955–969 (1967).
[19] W. D. Hayes and R. F. Probstein: "Hypersonic Flow Theory" Academic Press, New York and London (1959).
[20] J. A. Laurmann: "The Free Molecule Probe and Its Use for the Study of Leading Edge Flows", Phys. Fluids vol. 1, No. 6, 469–477 (1958).
[21] S. A. Schaaf, F. C. Hurlbut, L. Talbot and J. Aroesty: "Viscous Interaction Experiments at Low Reynolds Numbers", ARS Jour. 527–528, July (1959).
[22] H. T. Nagamatsu, J. A. Weil and R. E. Sheer Jr.: "Heat Transfer to Flat Plate in High Temperature Rarefied Ultrahigh Mach Number Flow", ARS Jour. 533–541, Apirl (1962).
[23] R. J. Vidal and C. E. Wittliff: "Hypersonic Law Density Studies of Blunt and Slender Bodies", Rarefied Gas Dynamics suppl. 2, vol. II, 348–378 (1963).
[24] R. L. Chuan and S. A. Waiter: "Experimental Study of Hypersonic Rarefied Flow near the Leading Edge of a Thin Flat Plate", Rarefied Gas Dynamics suppl. 2, vol. II, 328–342 (1963).
[25] Yu. A. Koshmarov and N. M. Gorskaya: "Heat Transfer and Equilibrium Temperature on a Thin Plate in Hypersonic Flow with Strong Interaction", Int. J. Heat and Mass Transfer vol. 8 1415–1420 (1965).
[26] J. E. Wallace and A. F. Burke: "An Experimental Study of Surface and Flow Field Effects in Hypersonic Low Density Flow over a Flat Plate", Rarefied Gas Dynamics suppl. 3, vol. I, 487–507 (1965).
[27] R. J. Vidal and J. A. Bartz: "Experimental Studies of Low-Density Effects in Hypersonic Wedge Flows", Rarefied Gas Dynamics suppl. 3, vol. I, 467–486 (1965).
[28] I. E. Vas, J. McDougall, G. Koppenwallner, and S. M. Bogdonoff: "Some Exploratory Experimental Studies of Hypersonic Low Density Effects on Flat Plates and Cones", Rarefied Gas Dynamics suppl. 3, vol. I, 508–534 (1965).
[29] W. J. McCroskey, S. M. Bogdonoff, and J. G. McDougall: "An Experimental Model for the Sharp Flat Plate in Rarefied Hypersonic Flow", AIAA Jour. vol. 4, No. 9, 1580–1587 (1966).
[30] W. J. McCroskey and J. G. McDougall: "Shock Wave Shapes on a Sharp Flat Plate in Rarefied Hypersonic Flow", AIAA Jour. vol. 4, No. 1, 184–186 (1966).
[31] W. J. McCroskey, S. M. Bogdonoff and A. P. Genchi: "Leading Edge Flow Studies of Sharp Bodies in Rarefied Hypersonic Flow", Rarefied Gas Dynamics suppl. 4, vol. II, 1047–1066 (1967).
[32] W. J. McCroskey: "Density and Velocity Measurements in High-Speed Flows", AIAA Jour. vol. 6, No. 9, 1805–1807 (1968).
[33] M. Becker and D. E. Boylan: "Experimetnal Flow Field Investigations Near the Sharp Leading Edge of a Cooled Flat Plate in a Hypervelocity, Low Density Flow", Rarefied Gas Dynamics suppl. 4, vol. II, 993–1014 (1967).
[34] I. E. Vas and J. Allegre: "The N-4 Hypersonic Low Density Facility and Some Preliminary Results on a Sharp Flat Plate", Rarefied Gas Dynamics suppl. 4, vol. II, 1015–1030 (1967).
[35] E. S. Moulic and G. J. Maslach: "Induced Pressure Measurements on a Sharp-Edged Insulated Flat Plate in Low Density Hypersonic Flow", Rarefied Gas Dynamics suppl. 4, vol. II, 971–992 (1967).
[36] P. J. Harbour and J. H. Lewis: "Preliminary Measurements of the Hypersonic Rarefied Flow Field on a Sharp Flat Plate Using an Electron Beam Probe", Rarefied Gas Dynamics suppl. 4, vol. II, 1031–1046 (1967).
[37] W. B. Bush: "On the Viscous Hypersonic Blunt Body Problem", J. Fluid Mech. vol. 20, 353–367 (1964).
[38] J. M. Grange, J. M. Klineberg and L. Lees: "Laminer Boundary-Layer Separation and Near-Wake Flow for a Smooth Blunt Body at Supersonic and Hypersonic Speeds", AIAA Jour. vol. 5, No. 6, 1089–1096 (1967).
[39] H. C. Kao: "Hypersonic Viscous Flow Near the Stagnation Streamline of a Blunt Body", AIAA Jour. vol. 2, No. 11, 1892–1897 and 1898–1906 (1964).
[40] P. Trepaud and E. A. Brun: "A Study of Wakes a Behind Cylinders in Free-Molecule Flow", Rarefied Gas Dynamics suppl. 4, vol. II, 1177–1192 (1967).

[41] K. Tamada and K. Yamamoto: "Flow of Rarefied Gas past a Circular Cylinder at Low Mach Numbers", Reprinted from the Memoirs of the Faculty of Engineering, Kyoto University, vol. 30, Part 2, April (1968).
[42] J. L. Potter and A. B. Bailey: "Pressures in the Stagnation Regions of Blunt Bodies in Rarefied Flow", AIAA Jour. vol. 2, No. 4, 743–745 (1964).
[43] C. F. Dewey Jr. "Hot Wire Measurements in Low Reynolds Number Hypersonic Flows", ARS Jour. 1709–1718, December (1961).
[44] D. Tirumalesa: "An Experimental Study of Hypersonic Rarefied Flow over a Blunt Body", AIAA Jour. vol. 6, No. 2, 369–370 (1968).
[45] M. Hinada: "Experimental Study on the Drag of Blunt Bodies of Revolution at Hypersonic Speeds", ISAS Rept. No. 432, (vol. 33, No. 14) (1968).
[46] H. Coudeville, P. Trepaud, and E. A. Brun: "Drag Measurements in Slip and Transition Flow", Rarefied Gas Dynamics suppl. 3, vol. I, 444–466 (1965).
[47] R. N. Zapata, J. Haas, and G. K. Mruk: "Low Reynold Number Effects on Hypersonic Flow over a Two-Dimensional Cylinder", Rarefied Gas Dynamics suppl. 4, Vol. II, 1161–1176 (1967).
[48] J. E. Broadwell and H. Rungaldier: "Structure of the Shock Layer on Cylinders in Rarefied Gas Flow", Rarefied Gas Dynamics suppl. 4, vol. II, 1145–1160 (1967).
[49] J. P. Dawson and J. D. Haygood: "Cryopumping", Cryogenics vol 5, No. 2, 57–67, April (1965).
[50] G. D. Arney Jr. and A. B. Bailey: "Effect of Temperature on Pressure Measurements", AIAA Jour. vol. I, No. 12, 2863–2864 (1963).
[51] J. L. Potter, M. Kinslow, and D. E. Boylan: "An Influence of the Orifice on Measured Pressures in Rarefied Flow", Rarefied Gas Dynamics suppl. 3, vol. II, 175–194 (1965).
[52] L. Talbot: "Criterion for Slip Near the Leading Edge of a Flat Plate in Hypersonic Flow", AIAA Jour. vol. I, No. 5, 1169–1171 (1963).
[53] A. A. Sonin: "The Free Molecule Langmuir Probe and Its Use in Flow Field Studies", AIAA Paper No. 66–5 (1966).
[54] J. Laframboise: "Theory of Cylindrical and Spherical Langmuir Probes in a Collisionless Plasma at Rest", Rarefied Gas Dynamics suppl. 3, vol. II, 22–44 (1965).
[55] G. N. Patterson: "Molecular Flow of Gases", John Wiley, New York (1956).
[56] Y. Kobayashi and K. Oshima: "Hypersonic Rarefied Gas Flow Around a Cylinder", ISAS Rept. vol. 4, No. 1(A), 19–25 (1968).
[57] Y. Kobayashi, K. Oshima and K. Sugaya: "Experimental Study of Rocket Exhaust into the Vacuum", Japan Soc. Aero. and Space Scie. vol. 16, No. 177, 366–370 (1968).
[58] Chung-Yen Liu and L. Lees: "Kinetic Theory Description of Plane Compressible Couette Flow", Rarefied Gas Dynamics suppl. I, 391–428 (1961).
[59] P. L. Chambre and S. A. Schaaf: "The Theory of the Impact Tube at Low Pressures", Jour. Aero. Sci. vol. 15, No. 7, 735–737 (1948).
[60] A. K. Sreekanth: "Experiments on Impact Probes in a Rarefied Subsonic Gas Stream", AIAA Jour. vol. 6, No. 5, 927–929 (1968).
[61] J. Laufer and R. McClellan: "Measurements of Heat Transfer from Fine Wires in Supersonic Flows", J. Fluid Phys. 276–289 (1965).
[62] J. R. Stalder and D. Jukoff: "Heat Transfer to Bodies Traveling at High Speed in the Upper Atmosphree", Jour. Aero. Sci. vol. 15, No. 7, 381–391 (1948).
[63] E. L. Harris and G. N. Patterson: "Properties of Impact Pressure Probes in Free Molecule Flow", UTIA Rept. No. 52, April (1958).
[64] J. H. de Leeuw and D. E. Rothe: "A Numerical Solution for the Free-Molecule Impact-Pressure Probe Relations for Tubes of Arbitrary Length", UTIA Rept. No. 88, December (1962).